Chapter 3

Laser Prepared Thin Films for Optoelectronic Applications

Marcela Socol, Gabriel Socol, Nicoleta Preda, Anca Stanculescu and Florin Stanculescu

Additional information is available at the end of the chapter

http://dx.doi.org/10.5772/67659

Abstract

Laser techniques such as pulsed laser deposition, combinatorial pulsed laser deposition, and matrix-assisted pulsed laser evaporation were used to deposit thin films for optoelectronic applications. High-quality transparent conductor oxide films ITO, AZO, and IZO were deposited on polyethylene terephthalate by PLD, an important experimental parameter being the target-substrate distance. The TCO films present a high transparency (>95%) and a reduced electrical resistivity (5×10^{-4} Ωcm) characteristics very useful for their integration in the flexible electronics. $In_xZn_{1-x}O$ films with a compositional library were obtained by CPLD. These films are featured by a high optical transmission (>95%), the lowest resistivity (8.6×10^{-4} Ωcm) being observed for an indium content of about 44–49 at.%. Organic heterostructures based on arylenevinylene oligomers (P78 and P13) or arylene polymers (AMC16 and AMC22) were obtained by MAPLE. In the case of ITO/P78/Alq3/Al heterostructures, a higher current value is obtained when the film thickness increases. Also, a photovoltaic effect was observed for heterostructures based on AMC16 or AMC22 deposited on ITO covered by a thin layer of PEDOT:PSS. Due to their optical and electrical properties, such organic heterostructures can be interesting for the organic photovoltaic cells (OPV) applications.

Keywords: PLD, CPLD, TCO, MAPLE, organic thin films

1. Introduction

During the time, the deposition methods have been developed or/and adapted to process materials with special properties as thin films. It is well known that between the deposition methods and the quality of the obtained layers exist a strong correlation.

From the actual deposition techniques, those based on laser prove their great potential in the field of the thin films processing for different applications. Moreover, the methods based on pulsed laser have been widely implied in the preparation of transparent conductor oxide (TCO), organic films, nitrides, biomaterials, etc. [1–4].

TCO are materials integrated in applications such as organic photovoltaic cells (OPV), organic light-emitting devices (OLED), organic field-effect transistors (OFET), or smart windows [5–8]. Generally, in order to be used in optoelectronic applications, these materials must satisfy special requirements such as high optical transmittance in visible parts of the spectrum, significant reflectance in IR, and a reduced electrical resistivity [9, 10]. The most used TCO is indium tin oxide (ITO) based on indium, a rare and expensive material, deposited on glass or flexible substrates [1, 5]. Beside ITO, other TCO material used is ZnO, especially ZnO doped with elements from the III group as aluminum, indium, or gallium for improving its conductivity [11–13]. It was reported that using an aluminum-doped zinc oxide (AZO) electrode, which has absorption under 380 nm, can avoid the degradation of the cell due to the UV irradiation in the OPV applications [14]. Indium zinc oxide (IZO) films are characterized by a high electrical mobility and increased carrier density [15, 16].

Organics are a class of materials containing a large variety of compounds as small molecules, oligomers, and polymers that, lately, have been intensively studied in order to replace the inorganic materials in different domains. The most important applications of the organic semiconductors are OPV, OLED, and OFET [17–19]. Thus, Heliatek reported that a higher efficiency (13.2%) can be obtained in the field of the organic materials using a combination of the three oligomers [20]. Organic light-emitting devices are already implemented in applications as displays (in TV sets or in mobile phone) and lighting sources. OFET are used in the sensor applications [21]. A great advantage of these organic materials comes from the facts that they are ecofriendly and at low cost fabricated by a large variety of deposition techniques.

In this chapter, some of our contributions in the field of the TCO layers and organic thin films deposited by laser techniques (pulsed laser deposition (PLD), combinatorial pulsed laser deposition (CPLD), and matrix-assisted pulsed laser evaporation (MAPLE)) are presented. All these materials have been studied to be further integrated into OPV applications: TCO (ITO, AZO, and IZO) as transparent electrodes (anode) and organic semiconductors as active layers. The TCO materials obtained by PLD and CPLD present suitable optical and electrical properties as high transparency and reduced electrical resistivity. The MAPLE prepared organic films are characterized by a large absorption domain and adequate electrical properties.

2. Insights into the laser-based techniques for deposition of thin films—basic principles and experimental set-ups

Various deposition methods based on chemical or physical processes are used to obtain different materials in thin films form. The technique is chosen to obtain coatings with the expected

http://dx.doi.org/10.5772/67659

properties for targeted applications, by tuning the parameters implied in the deposition process. In the field of OPV applications, the requested TCO can be obtained using methods such as RF magnetron sputtering, oxygen ion beam-assisted deposition, spray chemical vapor deposition (CVD), PLD, and spray pyrolysis [22–26].

For the preparation of the organic active layer, methods such as vacuum thermal evaporation, spin-coating, Langmuir-Blodgett, inkjet printing, and MAPLE can be used [27–31].

In the following are briefly summarized the laser methods used in our work for the preparation of TCO and organic layers, to understand their basic principles, and the way in which the appropriate technique can be chosen in order to obtain layers with adequate properties.

2.1. Pulsed laser deposition (PLD)

PLD is a deposition technique widely used in the preparations of the thin films based on material or on combination of materials. High-quality coatings with special properties can be performed by PLD. Materials with complicated composition can be transferred by PLD on substrate without changing their stoichiometry [3]. During the material transfer process, a high-intensity laser source falls on a solid target containing materials used for deposition inside a vacuum chamber or filled with inert gas as nitrogen (N_2) or reactive gas as oxygen (O_2). Over a particular value of the incident laser intensity, the target elements are heated above their evaporation temperature (evaporation threshold). The materials are ejected from the target forming the plasma plume and moved toward the substrate. The plasma species that have sufficient energy condenses on the substrate producing the nucleation and the thin film grow up [32]. The target is rotated in order to prevent the local deterioration, which can affect the uniformity and quality of the obtained coating. A typical PLD experimental set-up is presented in **Figure 1**. Into a PLD process, the most important parameters are laser fluence, deposition rate, substrate temperature, target-substrate distance, and number of laser pulses [33].

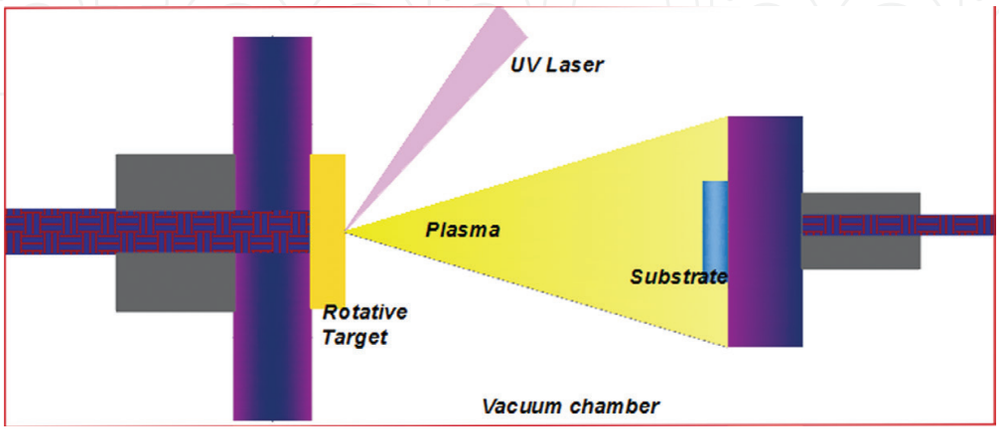

Figure 1. Schematic representation of PLD set-up.

2.2. Combinatorial pulsed laser deposition (CPLD)

In the beginning, the CPLD was introduced, in chemistry, in the fields of drugs from the necessity to develop new active molecules [34, 35], but this technique can be applied for a variety of materials: metals, semiconductors, polymers [36–38], etc. This deposition method is a proper tool to obtain doped materials like TCO layers.

The great advantage of the CPLD over PLD is the possibility to perform in a single experiment samples with different composition. By comparison, in order to find the sample with the best properties using PLD technique, it is necessary to carry out a lot of samples with different compositions; a time-consuming process using CPLD is obtained, a so-called composition library. Practically, along the deposition substrate in each point, the concentration of the thin films is different. In **Figure 2**, a CPLD deposition set-up is illustrated. In comparison with the PLD, in the CPLD deposition process is involved targets with different composition, situated at certain distance to each other [39]. An optical beam-splitter is used to split the laser beam into two beams. The targets are simultaneously ablated, generating intermixed films [40].

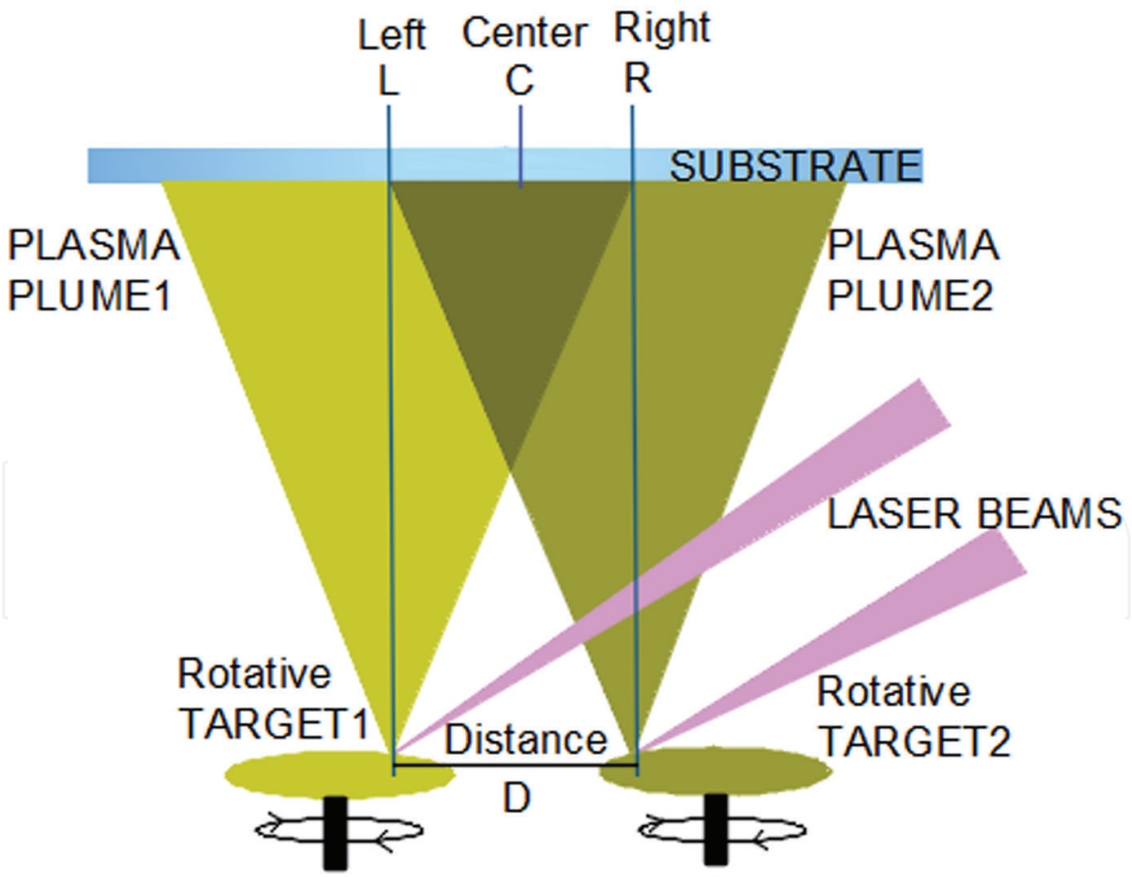

Figure 2. Schematic representation of CPLD set-up.

http://dx.doi.org/10.5772/67659

2.3. Matrix-assisted pulsed laser evaporation (MAPLE)

This technique is also derived from PLD method; Piqué et al. [41] mentioned that this technique was first introduced by Epstein in 1997 [42]. MAPLE has the advantage that it can process soft materials (organics) that could not be transferred by other techniques because there is the risk that takes place—a decomposition of the materials. In MAPLE, the target is formed from the materials (one or more) that must be deposited, and an adequate solvent is used as matrix [43, 44]. The solvent is chosen to obtain a homogeneous mixture (concentration usually below 3%) and to be compatible with the used laser wavelength. The formed mixture (organic material and solvent) is subsequently frozen in liquid nitrogen to form a solid target. During the deposition, the laser energy is absorbed by the solvent and transformed into thermal energy, enabling the evaporation of the solvent, and this being pumped away by the vacuum system while the material of interest reaches the substrate [45–47].

In MAPLE, smaller fluence are used (under 0.5 J/cm^2) in order to prevent the deterioration of the materials [44]. Another great advantage compared with methods used for the deposition of the organic materials is the possibility to obtain stacked layers without deterioration of the preliminary deposited layer [31]. **Figure 3** presents a schematic representation of the experimental set-up used in MAPLE deposition.

In **Table 1**, are presented comparatively the pulsed laser techniques described before which can be used to prepare thin films from different materials with thickness from nano to micrometers.

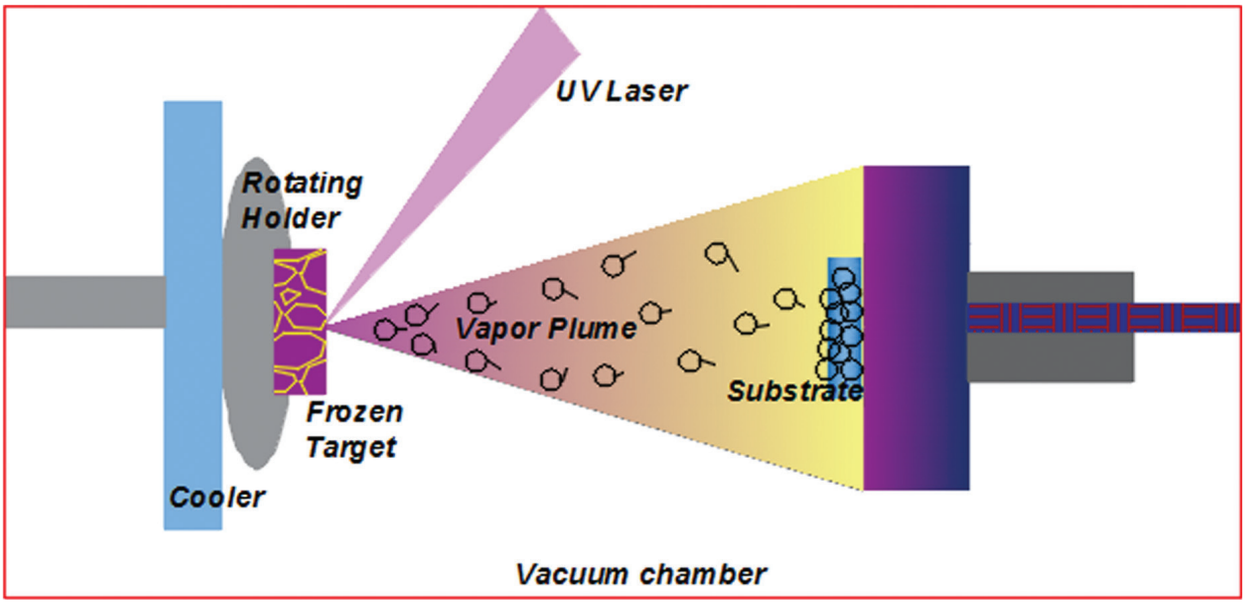

Figure 3. Schematic representation of MAPLE set-up used for the deposition of organic films.

Method	PLD	CPLD	MAPLE
Class of materials	Suitable for any inorganic material with complex and very complex stoichiometry	Combination of any inorganic materials	Suitable for deposition of organic compounds and laser transfer of inorganic or organic nanostructures (e.g., nanoparticles, nanotubes, nano-sheets, etc.)
Typical laser fluences (J/cm^2)	1–10	1–10	0.05–0.5
Principle of the laser transfer	Laser ablation of solid targets	Laser ablation of solid targets with different composition	Laser evaporation of frozen composite targets under ablation threshold
Deposition rate (nm/pulse)	0.01–0.5	0.01–0.5	0.1–0.5
Typical film thickness (nm)	1–5000	10–1000	10–5000

Table 1. Advantages of pulsed laser techniques for deposition of thin films.

3. Transparent conductive oxide (TCO) thin films deposited by PLD or CPLD—influence of the deposition conditions on their structural, morphological, optical, and electrical properties

The great interest in the field of TCO is proved by the high number of the research articles, reviews, books, or chapter books existent in the literature regarding this topic [48–56]. Various attempts were made to find the TCO with high optical and electrical properties and the best method to obtain these properties. The first TCO preparation is attributed to Badeker and dates from 1907, when CdO was obtained by the thermal oxidation of a Cd film deposited by sputtering [57]. ITO was frequently used in different applications, being one of the most-studied materials. In time, materials such as In_2O_3, CdO, ZnO, and SnO_2 were also addressed as TCO. n type semiconductors can be doped in order to improve their electrical conductivity, obtaining materials such as In_2O_3-ZnO, In_2O_3-SnO_2, Ga_2O_3-In_2O_3, In_2O_3-$MgInO_4$, $ZnSnO_3$-$ZnIn_2O_5$, $ZnIn_2O_5$-$GaInO_3$, or $MgIn_2O_4$-$Zn_2In_2O_5$ [58]. Several attempts were made to prepare p type semiconductors: $CuGaO_2$, $SrCu_2O_2$, $CuAl_2O_2$, and $CuCrO_2$ [59–62].

There are many studies regarding the TCO prepared by PLD, the best result being reported for ITO thin films (7.2×10^{-5} Ωcm electrical resistivity and ~90% transparency [63]). Also, by PLD, ITO layers with a smooth surface (root mean square (RMS) ~ 4.5 Å) were obtained [64]. The performances of the ITO deposited by PLD are superior to that presented by commercially available ITO deposited by sputtering.

The TCO film represents a key element in all applications, including OPV, due to the fact that through this electrode passes the light depending on its optical transmittance [65].

Our results regarding the TCO films obtained by PLD and CPLD and their complex characterization by techniques such as X-ray diffraction (XRD), ultraviolet-visible spectroscopy (UV-VIS) and atomic force microscopy (AFM) are presented in the next section.

http://dx.doi.org/10.5772/67659

3.1. Indium tin oxide (ITO)

This material was the subject of many research studies and is the most used electrode in OPV applications because it seems to present the best electrical conductivity and optical properties. It is used as hole injector material, having a work function between 4.5 and 5 eV [33].

Because of the technological progress in the field of flexible electronics, light-weight and cheap TCO materials that are compatible with plastic substrates are necessary.

A PLD experimental set-up like that presented in **Figure 1** was used to prepare ITO thin films on polyethylene terephthalate (PET) substrate. An excimer laser with KrF* (model COMPex-Pro 205, Lambda Physics-Coherent), λ = 248 nm, and τ_{FWHM} = 25 nm was used to irradiate the ITO target (SCI engineered materials) in an ultrahigh vacuum chamber [1]. The depositions were made at room temperature, at 2 J/cm^2 laser fluence, and with 10 Hz repetition rate. The oxygen pressure was between 1 and 1.5 Pa. We have selected different deposition parameters: target-substrate distance (4, 6, or 8 cm) and the number of laser pulses (6000, 9000, or 12,000). The sample was labeled as ITO1 (4 cm distance and 6000 pulses), ITO2 (6 cm distance and 9000 pulses), and ITO3 (8 cm distance and 12,000 pulses).

Analyzing the ITO samples from the structural point of view (**Figure 4a**), it was found that the films present a lower crystallinity. The ITO1 film deposited at the lower target-substrate distance appears as a small and large peak at 35.2° corresponding to the (400) diffraction plane. An increase in the diffraction peak from 35.2° is remarked for the ITO2. A supplementary peak at ~30.2° (a reduced one) that corresponds to (222) diffraction plane of ITO [66] is also disclosed. The film ITO3 deposited at higher target-substrate distance is amorphous. This means that there is an optimum for the deposition condition for assuring an increased crystallinity of the ITO layer.

The UV-VIS spectra for ITO samples (**Figure 4b**) record subtracting the contribution of the flexible substrate and show the differences in the transmission degree. The sample ITO1 presents the lowest transparency (70–75%) that is being attributed to the presence of some defects (cracks) generated during a deposition process at this distance and the defects that scatter the light.

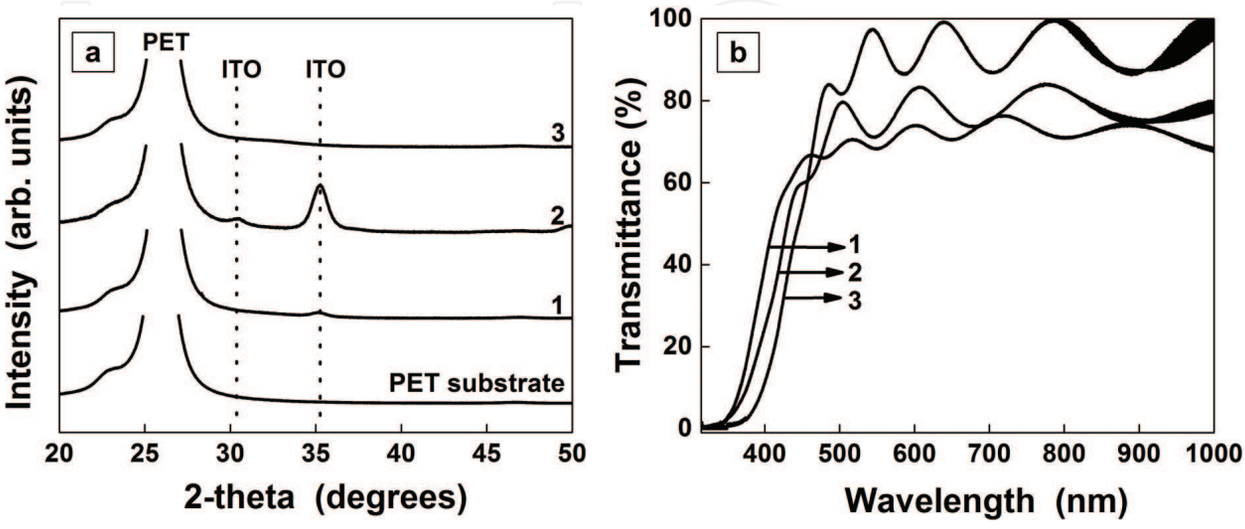

Figure 4. XRD patterns (a) and transmission spectra (b) of the ITO1, ITO2, and ITO3.

In PLD, the deposition appears as species with an increased kinetic energy that can affect the deposition substrate and the way in which this takes place is the nucleation process [1]. Defects can appear due to the energy transferred through the collision of the energetic items such as atoms, ions, and molecules, with the substrate atoms or with the atoms previously deposited. The adatoms must have enough time and mobility to form films with a good adherence at reduced substrate temperature [67].

The transmittance of the film increases with the increase of the target-substrate distance, reaching up to ~90% for the film deposited at a higher distance (ITO3).

Figure 5 shows the topographic images obtained by AFM. The appearance of the cracks in the ITO1 film can be observed. Also for the second sample, it was obtained morphologically with cracks. These cracks are characteristic to ITO deposited on PET substrates in some experimental conditions, which were being reported by the other authors also [68]. The smallest RMS value (2.4 nm) was obtained for the ITO3 film, compared to ITO1 (RMS = 15.5 nm) and to ITO2 (RMS = 31.5 nm), the ITO3 being the film showing the highest transmittance. This aspect of the sample is different from the other two, no cracks being observed on it.

In terms of the electrical resistivity, the sample ITO2 was measured with a good resistivity (5.9×10^{-4} Ωcm). Taking into account that this is the sample with the increased crystallinity, it can be concluded that there is a correlation between its crystallinity and its electrical properties. The sample ITO3 that is amorphous is featured by an increased resistivity (9.7×10^{-4} Ωcm). Higher value for the films is obtained by PLD at room temperature and had been reported by other authors [69]. The electrical properties of the TCO layers can be improved by heating the substrate is mentioned in the literature [70].

3.2. Aluminum-doped zinc oxide (AZO)

Another studied TCO with n type conduction is AZO, which is a nontoxic candidate having properties close to ITO. AZO samples were prepared by PLD on PET substrate in the same condition as ITO using a target with 2% Al content (SCI engineered materials). The samples prepared in different geometrical configuration were also labeled as AZO1 (4 cm), AZO2 (6 cm), and AZO3 (8 cm).

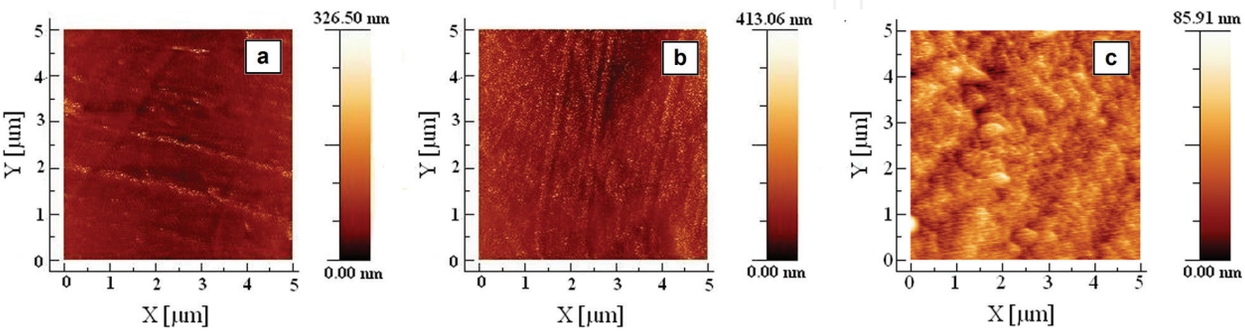

Figure 5. AFM images of the ITO1 (a), ITO2 (b), and ITO3 (c).

http://dx.doi.org/10.5772/67659

As for ITO, defects like cracks were remarked on the AZO layers deposited at 4 cm target-substrate distance (AZO1) and at 6 cm (AZO2). Films with crystalline quality (**Figure 6a**) were obtained at 6 and 8 cm. All AZO samples show a diffraction peak situated at ~34°, corresponding to (002) plane of ZnO [71]. The broadening of this peak from 34° for AZO1 is attributed to the presence of the lattice strain in this film, resulting in a peeling effect of the flayer.

The UV-VIS spectra in **Figure 6b** can be observed has a higher transmittance (over 90%) obtained for AZO3 coating compared with AZO1 and AZO2. A high optical quality is achieved for the film obtained at 8 cm target-substrate distance because, after target ejection, probably the energetic species have enough time to be thermalized in collision with the oxygen molecule when the distance is increased between target and PET substrate.

The AZO films present a morphology with long aggregates (**Figure 7**). The AZO3 has the bigger aggregates (with size between 0.4 and 1 μm) that are oriented in the same direction. This is in concordance with the higher transmittance observed for this layer due to the reduction of the light scattering on the grain boundaries. The AZO2 film presents the morphology similarly to AZO3 but with smaller aggregates, the film having lower RMS value (5.2 nm) compared with AZO1 (RMS = 12.4 nm) and AZO3 (RMS = 8.5 nm).

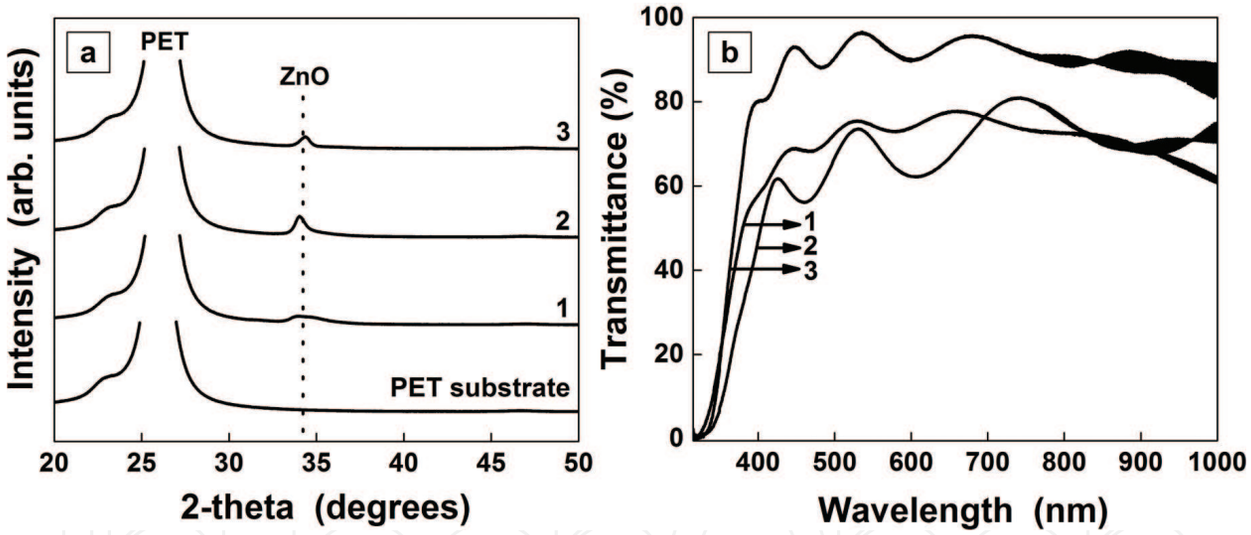

Figure 6. XRD patterns (a) and transmission spectra (b) of the AZO1, AZO2, and AZO3.

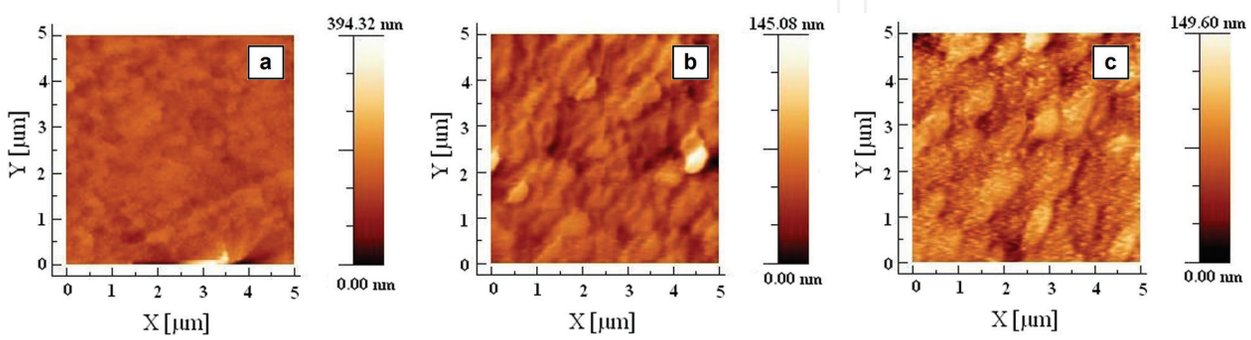

Figure 7. AFM images of the AZO1 (a), AZO2 (b), and AZO3 (c).

The best electrical resistivity (6.8×10^{-4} Ωcm) was found for the AZO2 film, with the AZO3 sample having increased in value (2.1×10^{-3} Ωcm). Due to the plasma expansion between target and substrate at a distance of 8 cm, it could appear that some oxidation effects affect the ZnO stoichiometry. Collisions and recombination can appear due to the oxygen background. Nevertheless, the resistivity values are better than other reported values (1.1×10^{-3} Ωcm) for AZO deposited on PET by RF magnetron sputtering at 100°C [72].

3.3. Indium zinc oxide (IZO)

Competitive optical and electrical properties were found for IZO electrode in comparison with that reported for ITO. IZO has a work function of ~5.2 eV being framed also as an n type semiconductor. The same deposition parameters used before were preserved to deposit IZO by PLD on PET from a solid target formed with In in atomic concentration, In/(In + Zn), of 70% by mixing In_2O_3 and ZnO powders (both from Aldrich). Also, in this case, the samples were labeled in accordance with the target-substrate distance: IZO1 (4 cm), IZO2 (6 cm), and IZO3 (8 cm).

As is reported in the literature [25], generally, IZO layers deposited at room temperature are amorphous (**Figure 8a**). A broad peak appears between 31 and 34° only for the IZO1 film. This peak contains two contributions one attributed to (111) diffraction plane of In_2O_3, which is usually situated ~31° and another to (101) diffraction plane of ZnO, which appears at 34° [25]. For the IZO1 and IZO2 layers, no diffraction peaks were observed.

If for the ITO and AZO, we have observed the appearance of a significant number of defects on the samples deposited at 4 and 6 cm, in the case of IZO, defects were evidenced just for the samples performed at the lower target-substrate distance (IZO1). For IZO layers, the transmittance is reduced compared with ITO and AZO (**Figure 8b**). No noticeable differences appear in the transmission spectra of the IZO films deposited at different target-substrate distances, the transmittance having between 75 and 88%.

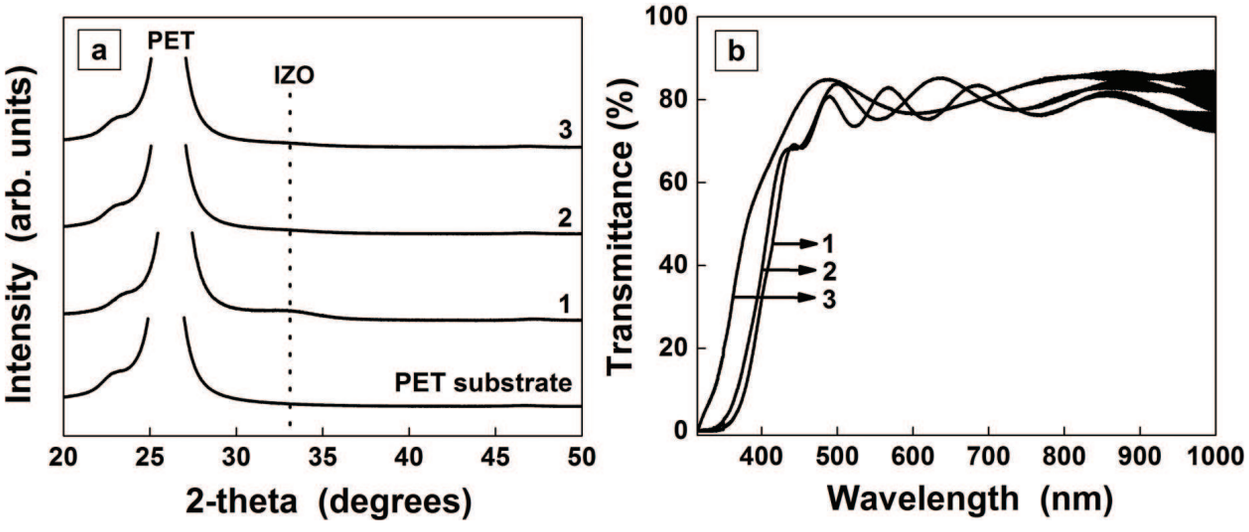

Figure 8. XRD patterns (a) and transmission spectra (b) of the IZO1, IZXO2, and IZO3.

http://dx.doi.org/10.5772/67659

The RMS values of the IZO films were evaluated by AFM (**Figure 9**). Thus, for the IZO3 sample, low RMS value (2.1 nm) was interpolated from AFM measurements. The other two films (IZO1 and IZO2) present higher RMS values (47.4 and 21.2 nm). The great value obtained for the IZO1 can be attributed to the presence of the cracks in this film. The best value for IZO3 is comparable with that obtained for ITO1. In order to be adequate for device applications, in addition to possess good optical and electrical properties, the films must be characterized by a smooth surface [33].

The resistivity values obtained for IZO samples were much better, compared with ITO and AZO layers, being ranged in 5.4–6.7 × 10^{-4} Ωcm domain. These values are in agreement with other results obtained for coatings made on glass substrate [25].

Considering all the investigated properties for ITO, AZO, and IZO deposited by PLD on the flexible substrate, it can be concluded that an important parameter in PLD process is the target-substrate distance. At a higher distance (8 cm) smooth films are obtained characterized by increased transmittances compared with the films obtained at 4 or 6 cm distance. Films with high transparency (over 95%) can be obtained by this laser technique.

As was already pointed, another technique to obtain TCO films is CPLD; this method allows to obtain doped films with a compositional gradient along the deposition substrate.

Using the same laser beam and a combinatorial geometry as that presented in **Figure 2**, IZO films at 3 J/cm^2 laser fluence were deposited. Two targets with atomic In concentration, In/(In + Zn), of 28 and 56 at.% or 42 and 70 at.% were made by mixing In_2O_3 and ZnO powders [73]. The combinatorial samples were obtained in 1 Pa oxygen atmosphere and at room temperature. The laser repetition rate was 10 HZ, and the number of pulses was 3000. Substrates for deposition were 26 × 76 mm microscope glass slides. The distance between the targets and substrate was 5 cm. In order to make a relevant comparison, samples from each target, but just by PLD, were also performed. The samples obtained by CPLD were IZOCMB1 (with 28% and 56%) and IZOCMB2 (with 42% and 70%). The sample produced by PLD are labeled as IZO1A (28%), IZO1B (56%), IZO2A(42%), and IZO2B(70%).

The UV-VIS spectra of the films deposited by PLD are presented in **Figure 10a**. The UV-VIS spectra of the combinatorial samples, IZOCMB1 presented in **Figure 10b** and IZOCMB2 presented in **Figure 10c**, were collected in three points corresponding to L, C,

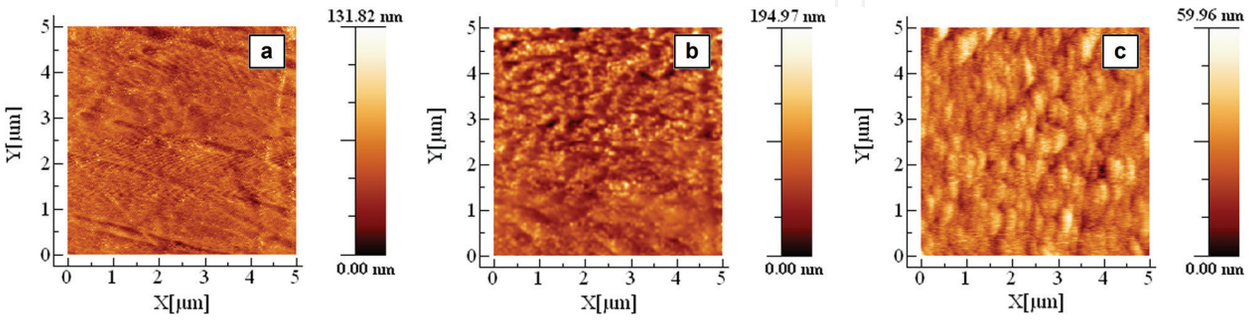

Figure 9. AFM images of the films deposited on PET substrate IZO1 (a), IZO2 (b), and IZO3 (c).

and R position (see **Figure 2**). The spectra are presented subtracting the glass contribution. Independently of the method used for deposition, PLD or CPLD, the samples show a high transmittance (up to 95%) in 500–1000 nm domain, which is a good premise for this TCO material.

For the films obtained by CPLD, a nonlinear variation in the composition of the films has been revealed by Energy dispersive X-ray spectroscopy (EDS) measurements (**Figure 11**). Data from 2.5 mm consecutive section along L-R line were mediated in order to establish the In, In/(In + Zn) content. Moreover, values from four areas were used to obtain the average In content from the target 1(TG1) and target 2 (TG2). We have obtained 28 and 56 at.% In, In/(In + Zn) atomic concentration for the first CPLD target and 42 and 70 at.% In, In/(In + Zn) for the second CPLD target. The films IZOCMB1 and IZOCMB2 have atomic concentration in In between L and R position, of 27–33 and 36–52 at.%, respectively. The lower In content is attributed to the ZnO preferential nucleation on glass substrate.

The AFM images obtained on the combinatorial films (in different areas between L and R points) are presented in **Figure 12**. The films are smooth, and the RMS roughness values are ranged between 7.1 and 26.2 nm for the IZOCMB1 film and 1.0 and 7.3 nm for the IZOCMB2 film.

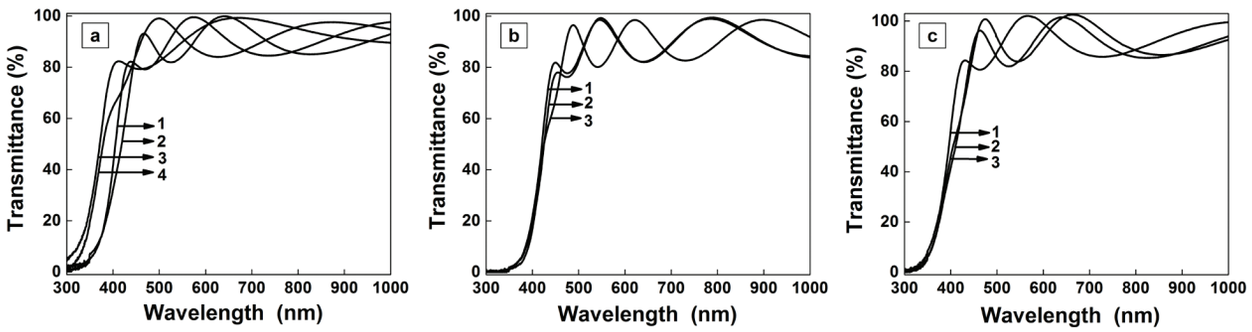

Figure 10. Transmission spectra of the IZO1A(curve1), IZO1B(curve2), IZO2A(curve3), IZO2B(curve4) (a) of the IZOCMB1 (b) and IZOCMB2 (c) in different areas corresponding to positions L, C, and R.

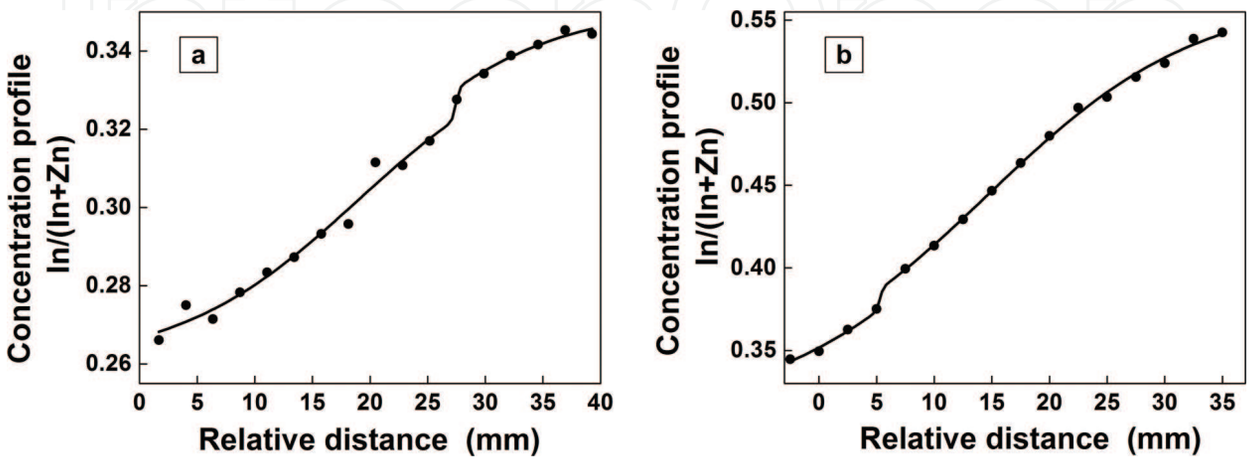

Figure 11. Elemental composition profiles of the IZO films deposited on glass substrate by CPLD using two targets with various In atomic concentration: (a) −28% (TG1) and 56% (TG2) and (b) −42% (TG1) and 70% (TG2).

http://dx.doi.org/10.5772/67659

The variation of RMS as a function by distance is given in **Figure 13**. The RMS mean value from three neighbor areas was used to plot each point in **Figure 13**. A decrease in the RMS value was observed with the increase in the In content between L and R points. This observation is in agreement with other results presented in the literature [74].

The modification of the electrical resistivity was also investigated along L-R direction of the films. The IZOCMB1 film presents a lower resistivity (2.3×10^{-3} Ωcm) for 28.8–29.5 at.% In content (**Figure 14a**), and IZOCMB2 film has a lower resistivity (8.6×10^{-4} Ωcm) in 44–49 at.% of In content region (**Figure 14b**). The literature reported similar data for the minimum resistivity obtained for samples with similar In atomic concentration deposited by magnetron sputtering [75, 76].

In conclusion, $In_xZn_{1-x}O$ ($27 \leq x \leq 52$) systems were performed by CPLD. The best resistivity value obtained was 8.6×10^{-4} Ωcm that correspond to 44–46 at.% In content domain. All investigated films present a high optical transparency (~95%). This technique is useful for preparing TCO films with different composition and adequate optical and electrical properties.

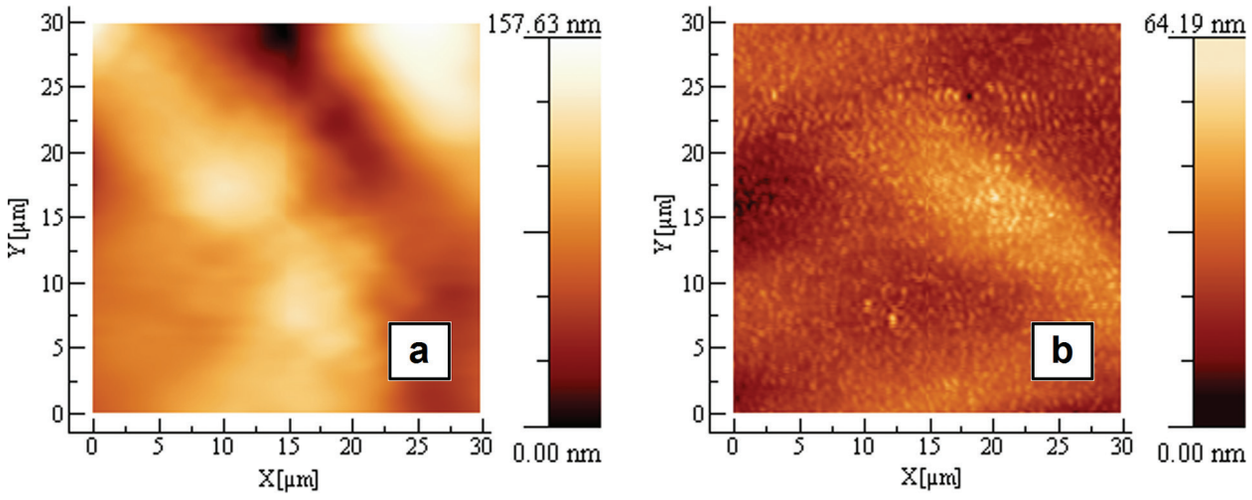

Figure 12. AFM images of IZOCMB1 (a) and IZOCMB2 (b).

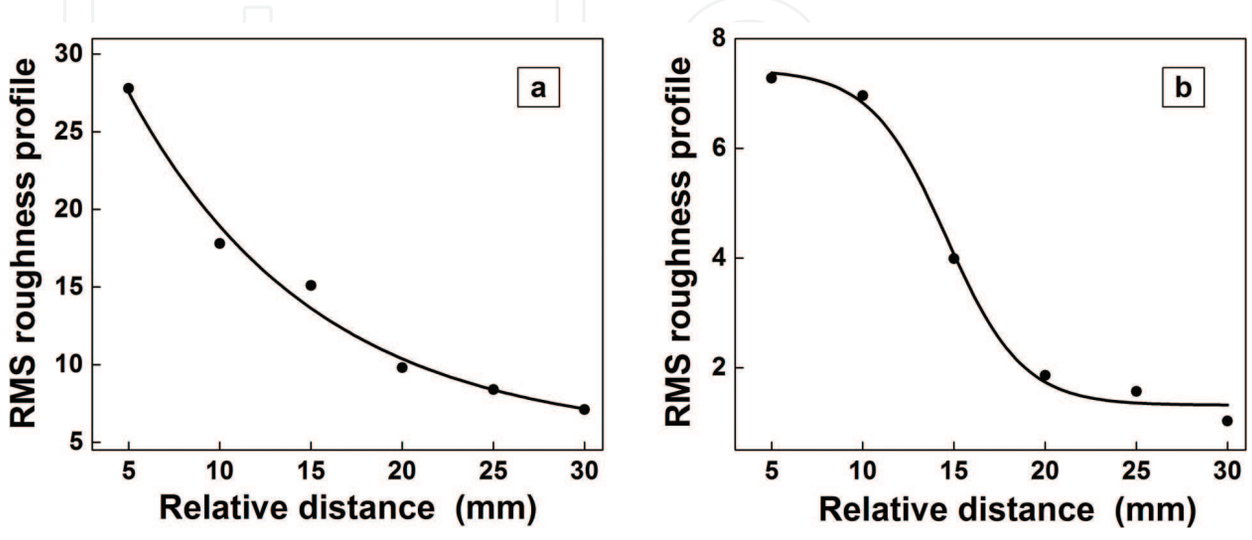

Figure 13. RMS roughness profiles of the IZOCMB1 (a) and IZOCMB2 (b) between L and R positions.

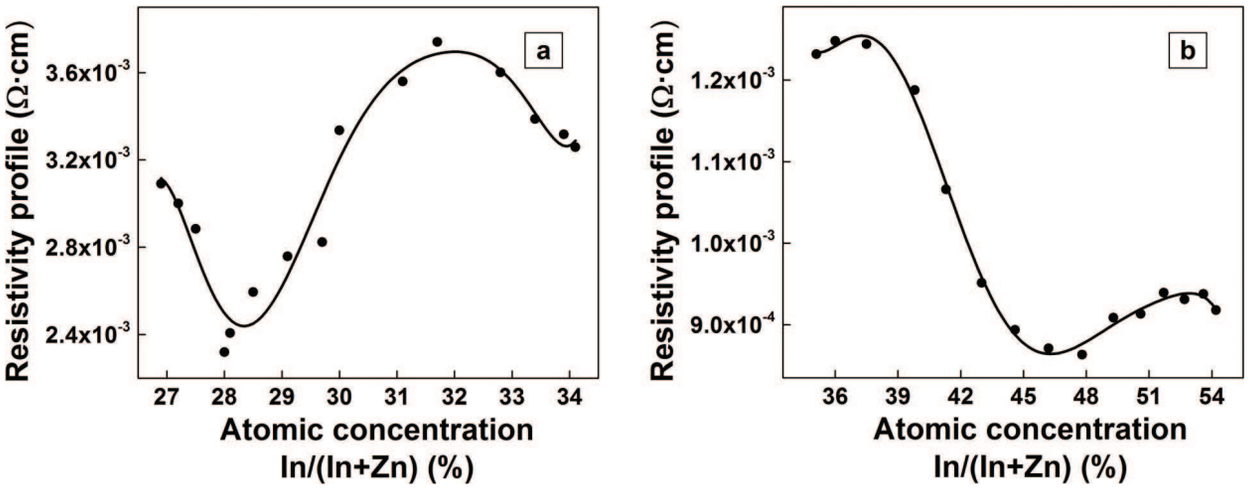

Figure 14. Electrical resistivity profiles of the IZOCMB1 (a) and IZOCMB2 (b).

4. Organic thin films deposited by MAPLE—properties and applications

At the same time with the development of the organic materials domain, a large number of deposition methods had been adapted to obtain them as thin films. The most used technique to deposit organic layers was vacuum evaporation, but for materials as oligomers or polymers, more suitable are techniques involving solution because the risk to destroy the molecular chains during the deposition is reduced. The spin-coating method was frequently used as deposition technique for the polymers thin films preparation.

In the last years, the MAPLE method was introduced in order to process such organic materials, taking into account that MAPLE allows their transfer with the preservation of their chemical composition.

Subsequently are presented the organic thin layers prepared by MAPLE. These were investigated from morphological (AFM) and optical (UV-VIS, photoluminescence spectroscopy—PL, Fourier transform infrared spectroscopy (FTIR), and from electrical (current-voltage characteristics) point of view.

4.1. Oligomers based on arylenevinylene compounds

Arylenevinylene oligomers, 1,4-*bis* [4-(N,N-diphenylamino)phenylvinyl] benzene (P78) and 3,3-*bis* (N-hexylcarbazole)vinylbenzene (P13), with electron-donating groups (triphenylamine and N-alkylcarbazole), are used in combination with *tris*(8-hydroxyquinolinato)aluminum salt (Alq_3) to prepare by MAPLE organic heterostructures with one or two layers. The molecular formula of the oligomers used in this study was presented in **Figure 15**. The concentration of the organic material in the dimethyl sulfoxide (DMSO), used as a solvent, was 2.5% (w/v). The depositions were made at 5 Hz laser frequency and at lower fluence (250 mJ/cm^2). In the heterostructures with two layers, the first deposited layer was the oligomer (P 13 or P78) and the second layer was Alq3 [77]. The number of laser pulses were 80,000 for 1P13, 1P78, and 1Alq3 samples and 160,000 for 2P13, 2P78, and 2Alq_3 samples.

http://dx.doi.org/10.5772/67659

The FTIR spectra (**Figure 16**) of the MAPLE-deposited layers have been analyzed and was concluded that no materials decomposition appear during the laser transfer. The peaks characteristic to P13 and P78 compounds were identified. The peak situated at 960 cm^{-1} is characteristic to HC=HC trans-out-of-plane bending vibration [78], whereas the δ (C-N) stretching vibration appears at 1154 cm^{-1} in P13 layer and at 1328 cm^{-1} in P78. The band from 1589 cm^{-1} in P78 is assigned to the vibration of the C-C phenyl group. The peaks from 1598 cm^{-1}, 1491 cm^{-1}, and 1477 cm^{-1} are due to the ν (C-C) vibration in monosubstituted benzene [78]. The Alq_3 layer presents vibration characteristic to the following chromophoric groups: between 600 and 900 cm^{-1} =C-H stretching, at 1475 cm^{-1} aromatic C=C stretching, at 1390 cm^{-1} C=N bond, at 1600 cm^{-1} the quinolinic ring [79].

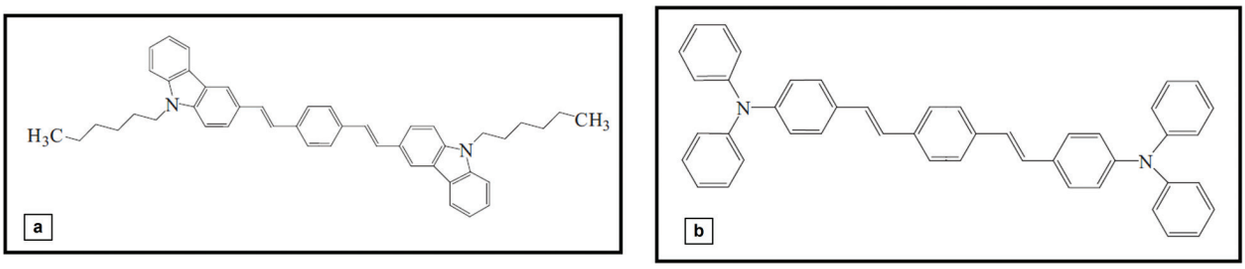

Figure 15. Chemical structures of the arylenevinylene oligomers: P13 (a) and P78 (b).

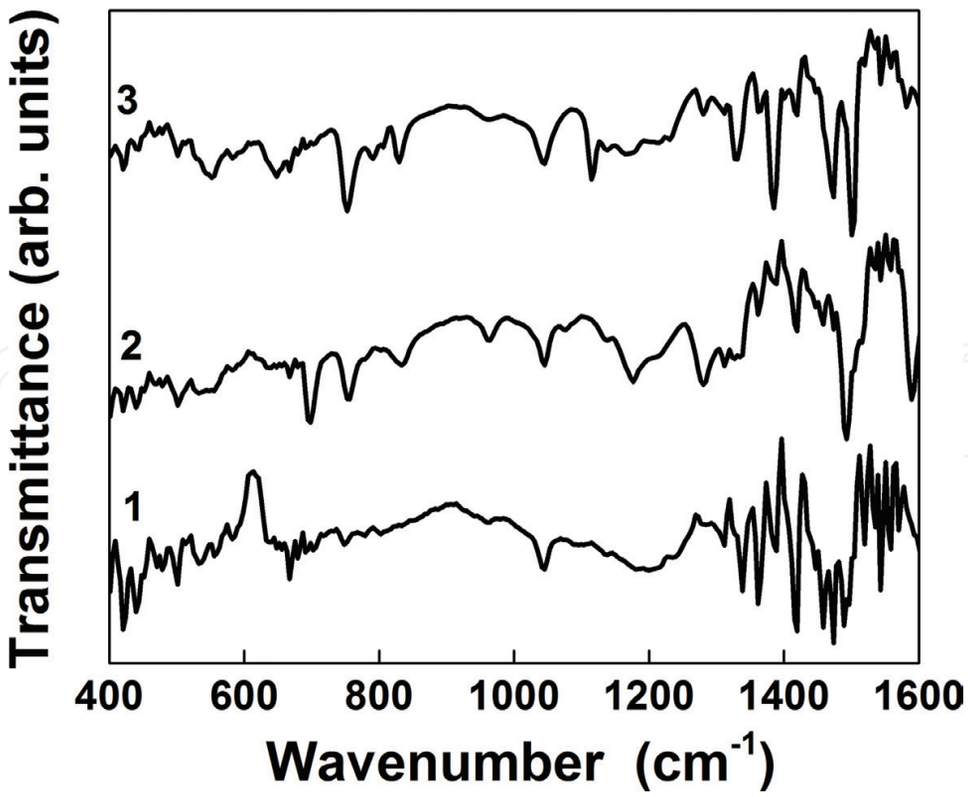

Figure 16. FTIR spectra of the organic thin films deposited on Si substrate by MAPLE: P13 (curve 1), P78 (curve 2), and Alq3 (curve 3).

The UV-VIS spectra of the P13 and P78 layers deposited by MAPLE on ITO and with an additional Alq_3 layer are presented in **Figure 17(a)** and **(b)**. The structures realized with two organic materials are featured by a great transparency, 60% for $\lambda > 550$ nm. Absorption maxima attributed to the electronic π-π^* transitions of the conjugated backbone [80] were evidenced. The absorption maxima characteristic to these materials and for the $Alq_{3,}$ situated at low wavelength are hidden by the ITO substrate [81].

The Alq_3 is frequently used in OLED applications due to its emission properties. The photoluminescence spectra of oligomers and Alq_3, obtained at 350 nm excitation wavelength are given in **Figure 17(c)** and **(d)**. The emission band with the maximum situated at 523 nm is attributed to the presence of the Alq_3 meridional stereoisomer [80]. P13 oligomer showed two emission maxima (490 and 525 nm), while P78 discloses a raw maxima at 500 nm [80], the prepared films preserving the emission properties of the start materials.

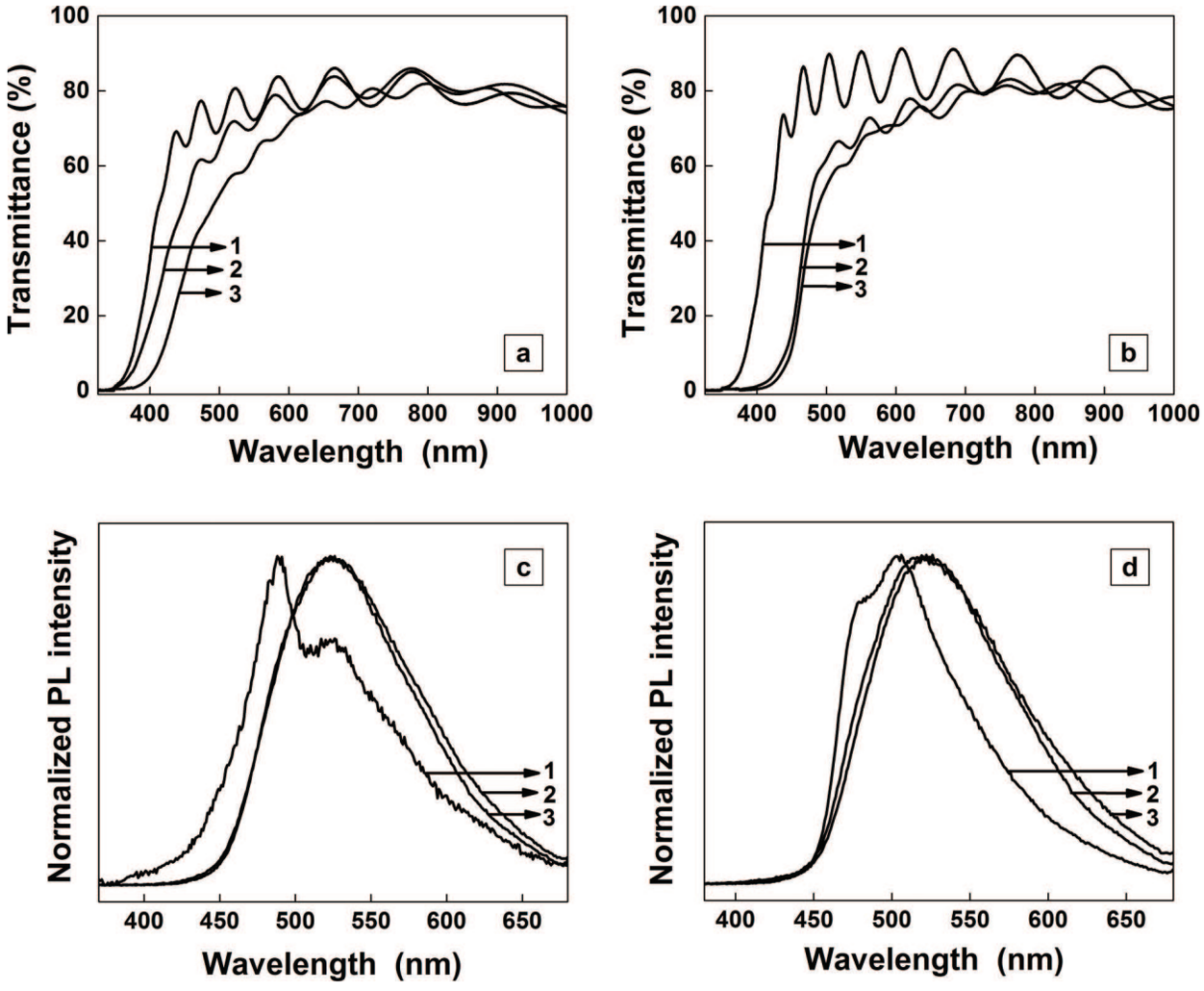

Figure 17. Transmission spectra (a, b) and photoluminescence spectra (c, d) of the organic thin films based on arylenevinylene oligomer (P13 (a, c) and P78 (b, d)) deposited on glass/ITO substrate by MAPLE. For transmission spectra: glass/ITO (curve 1), glass/ITO/arylenevinylene oligomer (curve 2), and glass/ITO/arylenevinylene oligomer/Alq3 (curve 3). For photoluminescence spectra: glass/ITO/arylenevinylene oligomer (curve 1), glass/ITO/Alq3 (curve 2), and glass/ITO/arylenevinylene oligomer/Alq3 (curve 3).

http://dx.doi.org/10.5772/67659

Different topographies of the films deposited by MAPLE are presented in **Figure 18**. The globular morphology is characteristic to MAPLE process [2, 11]. The RMS values obtained by interpolation of a single layer deposited on ITO evidenced that the P78 film (24.6 nm) presents a higher roughness compared with P13 (8.2 nm) (**Table 2**).

The samples made with a doubled number of pulses present RMS values comparable with that obtained for the samples realized with 80,000 laser pulses. A decrease in the RMS values was observed for the samples based on P78 and Alq_3 double layers, while an increase was seen for the sample containing P13 and Alq3 (**Table 2**). The higher roughness of P78 seems to favor a better fit of Alq_3 molecules.

The I-V characteristics recorded in 0–10 V domain in the dark are presented in **Figure 19**. No rectifying properties were observed for the investigated heterostructures. A good current value (8×10^{-6} A at 1 V) was evidenced in the sample based on P78 and Alq3 with thicker layers. The lowest current value was presented by the sample with Alq_3 layer realized at 160,000 laser pulses.

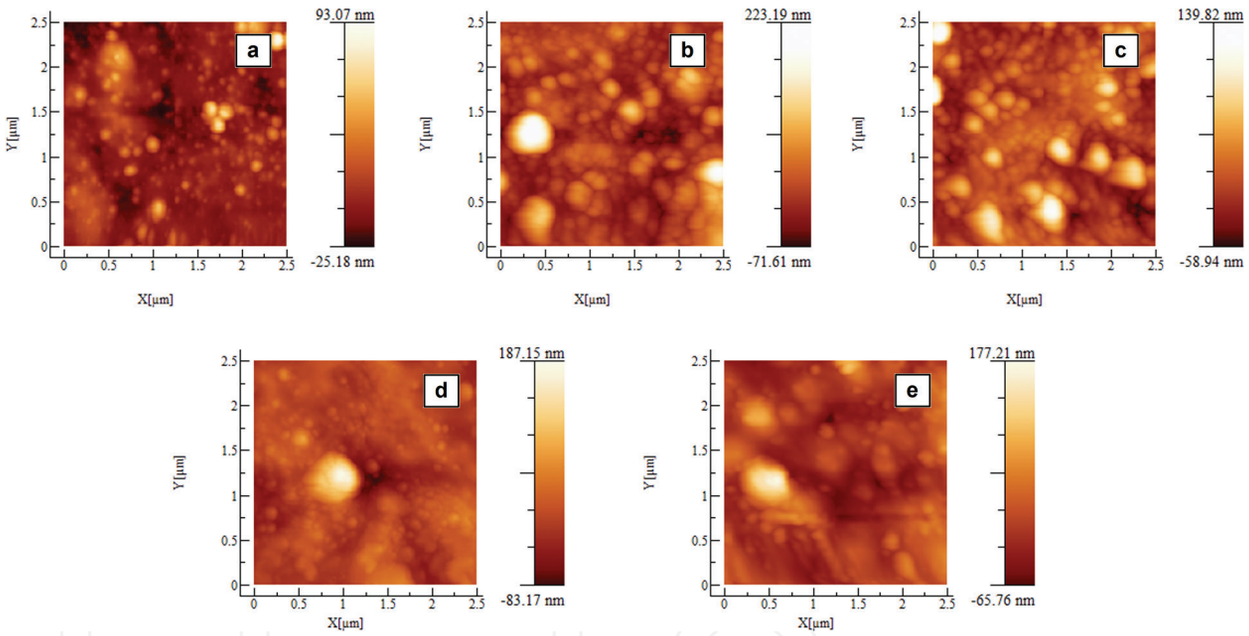

Figure 18. AFM images of the organic thin films deposited on glass/ITO substrate by MAPLE: glass/ITO/1P13 (a), glass/ITO/1P78 (b), glass/ITO/1Alq3 (c), glass/ITO/1P13/1Alq3 (d), and glass/ITO/1P78/1Alq3 (e).

Sample	RMS (nm)	Sample	RMS (nm)
1P78/ITO	35.3	1Alq3/1P13/ITO	26.2
1Alq3/1P78/ITO	31.8	2P13/ITO	12.6
2P78/ITO	36.2	2Alq3/2P13/ITO	28.5
2Alq3/2P78/ITO	29.1	1Alq3/ITO	26.0
1P13/ITO	10.4	2Alq3/ITO	30.1

Table 2. The RMS values obtained from the AFM on the organic thin films.

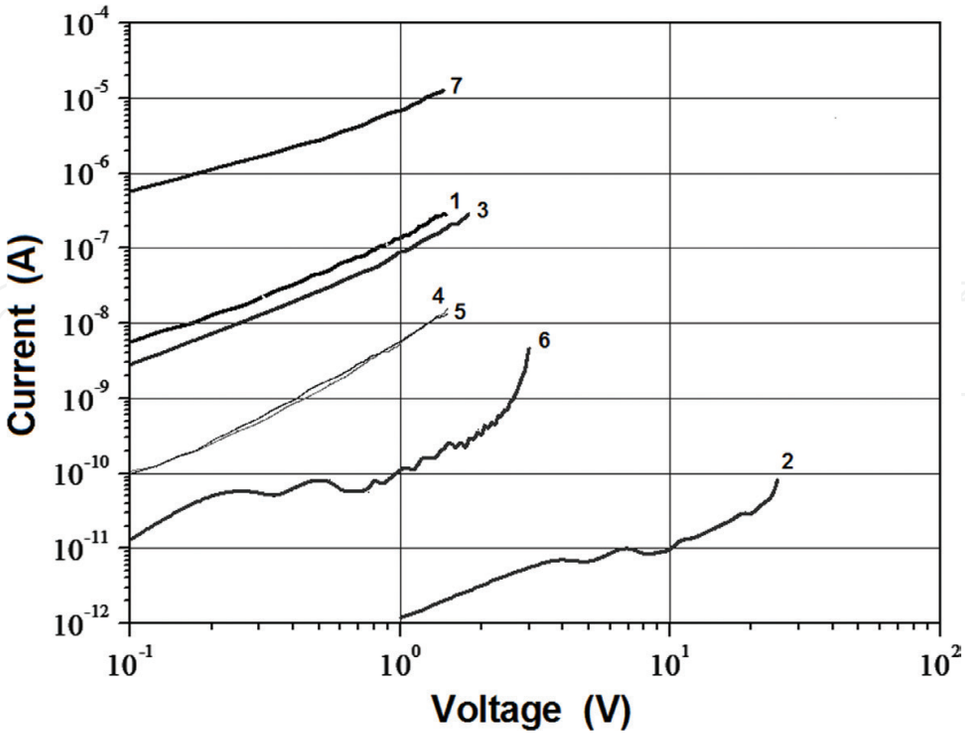

Figure 19. Current—voltage characteristics, in logarithmic representation, of the heterostructures based on arylenevinylene oligomer deposited on glass/ITO substrate by MAPLE using different no. of pulses (80,000 or 160,000): glass/ITO/Alq3/Al (curve 1—80,000 pulses, curve 2—160,000 pulses), glass/ITO/P13/Alq3/Al (curve 3—80,000 pulses, curve 4—160,000 pulses, curve 5—160,000 pulses, rev. bias), glass/ITO/P78/Alq3/Al (curve 6—80,000 pulses, curve 7—160,000 pulses).

Regarding the I-V characteristics of the heterostructures based on oligomers, it was remarked that their behavior is different. If, in the heterostructure with P78, a high current value was obtained for thicker layer (ITO/2P78/2Alq_3/Al), for the heterostructure with P13, the higher current value was recorded for thinner layers (ITO/1P13/1Alq_3/Al). No relevant changes are expected in the charge flow because there are no significant differences in the energetic barriers at IOT/P78 and ITO/P13 interfaces (**Figure 20**).

As was supposed by Gao [82], at the Al/Alq_3 interface, it can appear as a dipole layer, marked by a potential shift of −0.9 V, which determines a lowering of the Al cathode Fermi level to −5.2 eV, close to the Alq_3 HOMO level. The compounds have energy level positions that determine ohmic behavior or the appearance of the space charge limited currents (SCLC).

Analyzing at 1 V applied voltage, it is observed that in the heterostructure with Alq3 single layer formed with two layers, the current increases from 1.5×10^{-12} A for the ITO/2Alq_3/Al structure at 7×10^{-9} A and at 8×10^{-6} A for the ITO/2P13/2Alq_3/Al structure and for the ITO/2P78/2Alq_3/Al, respectively.

Thin films from oligomers and Alq_3 were deposited by MAPLE, and the films preserved the optical properties of the raw powders materials. In the heterostructure containing P78 and Alq_3 as stacked layers, the current value can be increased by using a thicker P78 layer.

http://dx.doi.org/10.5772/67659

4.2. Polymers based on arylene compounds

From the first generation of the organic photovoltaic cells realized with a single organic layer between anode and cathode [83], numerous attempts were made to improve the final cell parameters, either by developing new materials (as polymers with special properties) or using different cell architectures.

MAPLE method was used to obtain thin films from arylene-based polymers. The used polymers were poly[N-(2-ethylhexyl)2.7-carbazolyl vinylene]/AMC16 and poly[N-(2-ethylhexyl)2.7-carbazolyl 1.4-phenyleneethynylene]/AMC22 with the chemical structure presented in **Figure 21**. The same laser source mentioned above was used for the MAPLE deposition. The chloroform was used to obtain a target with 3 g/l concentration. We have deposited thin films on ITO, ITO covered with poly(3,4-ethylenedioxythiophene)-poly(styrenesulfonate) (PEDOT:PSS) and Si substrates in the following experimental conditions: 250 mJ/cm^2 laser fluence and 30,000 laser pulses [84].

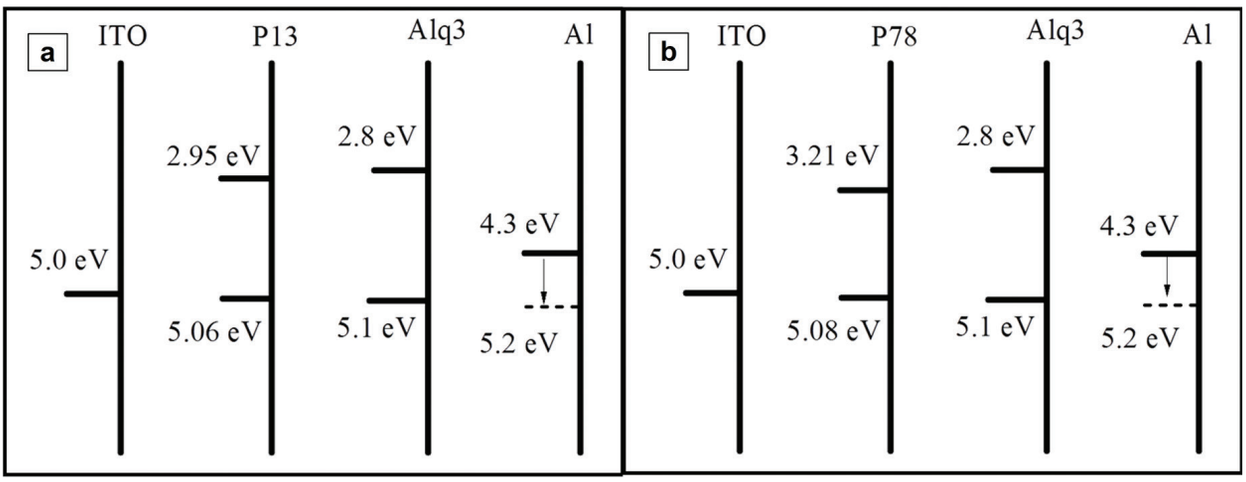

Figure 20. Band diagrams of the heterostructures based on arylenevinylene oligomer deposited on glass/ITO substrate by MAPLE: ITO/P13/Alq3/Al (a) and ITO/P78/Alq3/Al (b).

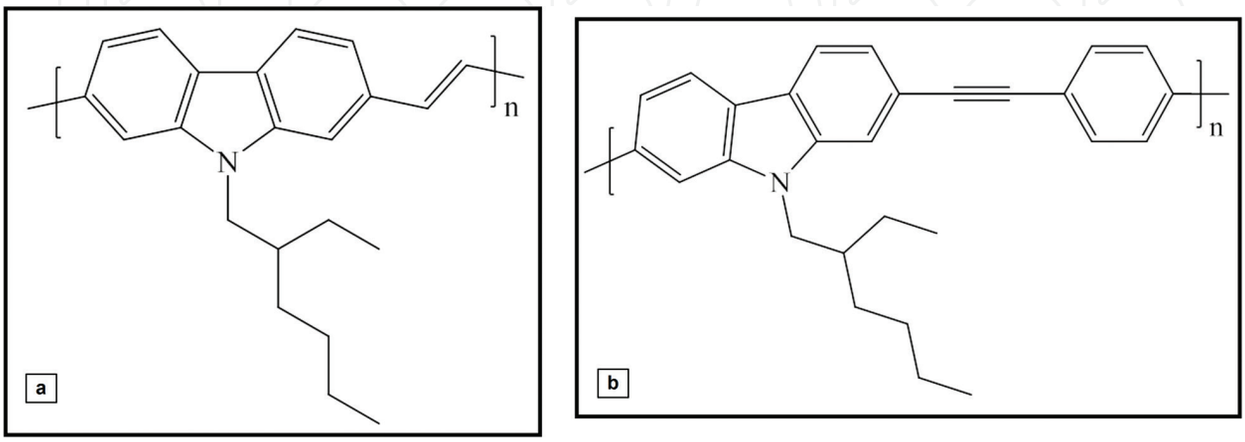

Figure 21. Chemical structures of the arylene polymers: AMC16 (a) and AMC22 (b).

The UV-VIS spectra (**Figure 22a**) and (**b**) of the organic film deposited by MAPLE were given in comparison with drop-cast realized films on glass substrate. A high transmittance is observed both for MAPLE films and for the drop-cast coatings (**Figure 22a**). The absence of the absorption maxima from 375 nm in the layers prepared by MAPLE (observed for the films deposited by drop-casting) is attributed to some modifications in the electronic structures of the polymeric films, determined by some differences in the arrangement of the molecules on the substrate surface. If for the preparing drop-cast film, the solvent is evaporated at room temperature, in MAPLE the solvent is thermally evaporated during the film deposition [85, 86]. Some cluster can appear, and this can affect the polymer backbone configuration [87, 88]. The polymers deposited by MAPLE on ITO and ITO/PEDOT:PSS (**Figure 22b**) exhibit a lower transmittance compared with the same layers prepared on glass.

The AFM images of the AMC 16 and AMC 22 films prepared by MAPLE on ITO and on ITO/PEDOT:PSS are given in **Figure 23**. The AMC22 polymer (with a reduced conjugated chain) forms layers with an increased roughness (RMS = 42 nm), when it is deposited on ITO/PEDOT:PSS substrate compared with the same layer deposited on ITO (RMS = 36 nm). In the case of AMC 16 with longer conjugated length, an increased roughness was obtained for the sample made on simple ITO substrate (RMS = 49.5 nm) compared with the sample realized on ITO/PEDOT:PSS substrate (RMS = 37 nm).

The I-V characteristics plotted in the dark and under illumination put into evidence the appearance of the photovoltaic effect in the polymeric films realized on ITO covered by an additional PEDOT:PSS layer (**Figure 24**). A higher current density (2.5×10^{-9} A/cm^2) was obtained in the dark at 0.5 V for the structure prepared with AMC 16 compared with that made with AMC 22 (~3×10^{-10} A/cm^2). The best photovoltaic parameters (open-circuit voltage-V_{OC}, short-circuit current-I_{SC}, and fill factor-FF) were shown by the cells based on AMC 16 ($V_{OC} = 0.303$, $I_{SC} = 12.7 \times 10^{-9}$ A, and FF = 29%) compared with the cell based on AMC22 ($V_{OC} = 0.073$, $I_{SC} = 8.2 \times 10^{-11}$ A, and

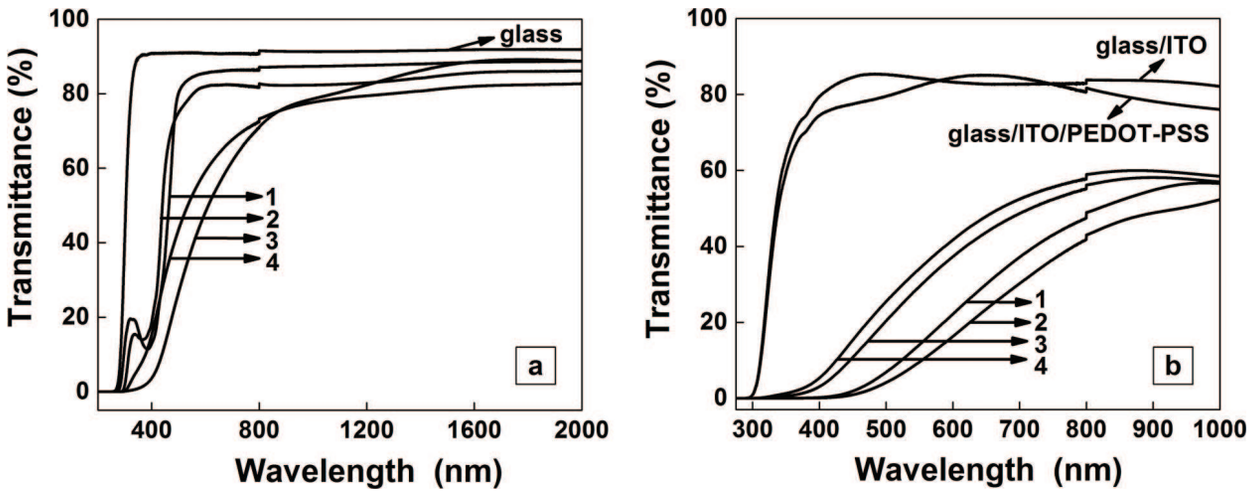

Figure 22. Transmission of the organic thin films based on arylene polymers (AMC16 and AMC22) deposited on glass (a), glass/ITO (b), and glass/ITO/PEDOT-PSS (b) substrates by drop-cast (only on glass) and MAPLE. On glass—AMC16 (curve 1—drop cast, curve 3) and AMC22 (curve 2—drop cast, curve 4), on glass/ITO—AMC16 (curve 1) and AMC22 (curve 3), on glass/ITO/PEDOT-PSS—AMC16 (curve 2) and AMC22 (curve 4).

http://dx.doi.org/10.5772/67659

FF = 25.9%). This sustains that a better collection of the charge appears in the cell structure realized with the polymer having a longer conjugation length. On the other hand, this is the sample with a lower roughness (RMS = 37 nm) of the active layer favoring the charge carrier transport.

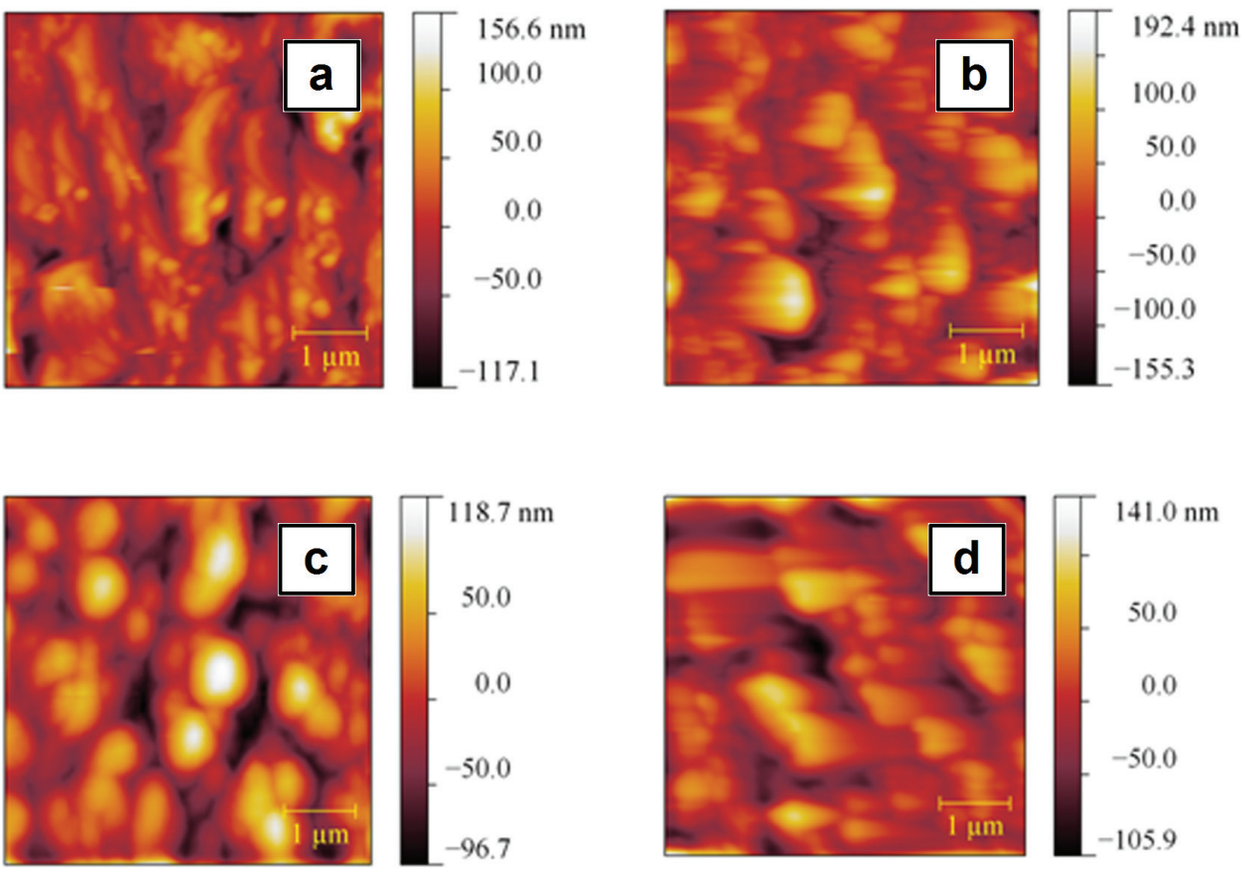

Figure 23. AFM images of the organic thin films deposited on glass/ITO (a, b) and glass/ITO/PEDOT-PSS (c, d) substrate by MAPLE: AMC16 (a, c) and AMC22 (b, d).

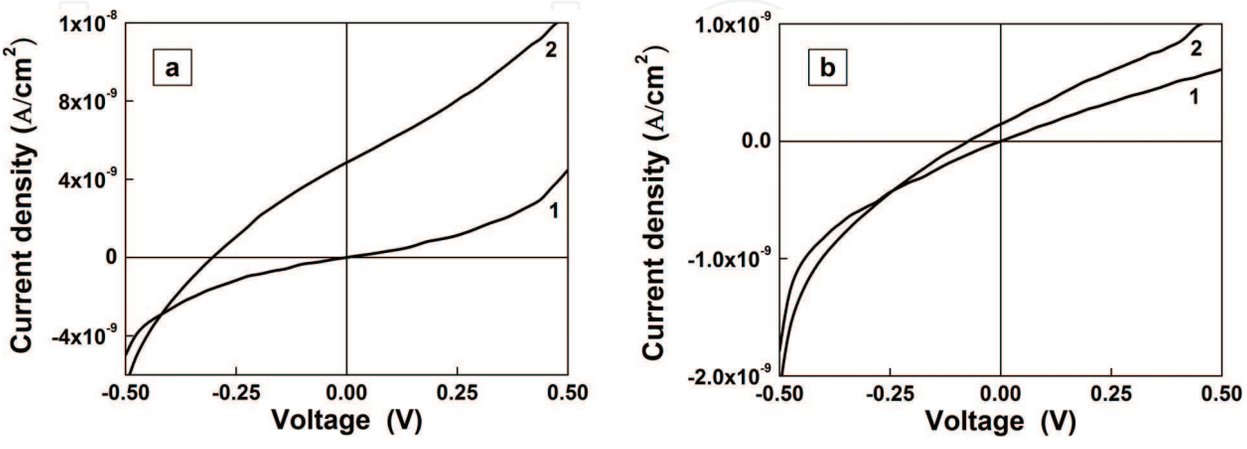

Figure 24. Current-voltage characteristics of the heterostructures based on arylene polymers deposited on glass/ITO/PEDOT-PSS substrate by MAPLE in dark (curves 1) and light (curves 2) conditions: glass/ITO/PEDOT-PSS/AMC16/Al (a) and glass/ITO/PEDOT-PSS/AMC22/Al (b).

Taking into account the presented results, it can be concluded that using MAPLE, polymeric thin films are deposited, characterized by good absorption in the blue-green region of the solar spectrum. The structures realized on ITO/PEDOT:PSS with AMC 16 and AMC 22 present photovoltaic effect, meaning that these materials can be taken into consideration for further applications in the OPV domain.

5. Conclusion

Summarizing, various thin films were deposited by PLD, CPLD, and MAPLE, the laser deposition technique being chosen in accordance with the material type (TCO or soft organic materials).

TCO films as ITO, AZO, and IZO are prepared by PLD on plastic substrate that presents a high transparency (~95%) and a reduced electrical resistivity (5×10^{-4} Ωcm), and the characteristics are very useful for integrating them in flexible electronics. An important parameter in the PLD experiments is the target-substrate distance. At a higher distance (8 cm), films free of cracks with a high transmittance and a reduced roughness were obtained. The exhibited electrical and optical properties are very good; all depositions were performed at room temperature without heating of the substrates.

$In_xZn_{1-x}O$ films were obtained by CPLD, using two targets with atomic In concentration In/(In + Zn), of 28 at.% and 56 at.% or 42 at.% and 70 at.%. The layers were analyzed from optical, electrical, and morphological point of view. We evidenced a high optical transmission, >95%. The lowest resistivity (8.6×10^{-4} Ωcm) was observed for an In content of about 44–49 at%. This technique is useful in the deposition of materials with different composition, each sample yielding practically a library of data, avoiding in this way the unnecessary loss of time. It is observed that the roughness of the samples decreases with the increase of the In content.

Layers based on arylenevinylene oligomers (P13, P78) and Alq3 were transferred by MAPLE without any material deterioration. Organic heterostructures with one or two organic layers were deposited. The optical properties of the start compounds were preserved. The prepared organic films present a good transmittance in the visible domain and the emission bands characteristic to the oligomers and to the Alq3. The globular morphology characteristic to MAPLE process was remarked. The I-V characteristics were symmetric, and the injector contact behavior was evidenced for the prepared heterostructures. For ITO/P78/Alq_3/Al heterostructures, the I-V plots evidenced dependence between the current value and the thickness of the organic layers.

Thin films from new arylene-based polymers were also processed by MAPLE. A good absorption was evidenced in the blue-green domain of the solar spectrum for the samples prepared with each polymer. The appearance of the photovoltaic effect was remarked for the heterostructures based on AMC16 film and AMC22 film deposited on ITO covered by a thin layer of PEDOT:PSS, which confirm that this buffer layer favors the charge carrier collection. The

heterostructure based on the polymer with longer conjugation length present the higher dark current density. Due to their optical and electrical properties, such organic heterostructures can be interesting for OPV applications.

Acknowledgements

The authors thank to the group from ICMPP Iasi (led by Dr. M. Grigoras) for the synthesis of the oligomers and of the polymers. The work has been funded by the Romanian National Authority for Scientific Research, CNCS-UEFISCDI, projects TE 188/2014, PN-II-RU-TE-2014-4-1590 and the National Authority for Research and Innovation in the frame of Core Program - contract 4N/2016 and contract PN16-480102.

Author details

Marcela Socol[1]*, Gabriel Socol[2], Nicoleta Preda[1], Anca Stanculescu[1] and Florin Stanculescu[3]

*Address all correspondence to: marcela.socol@infim.ro

1 National Institute of Material Physics, Bucharest-Magurele, Romania

2 National Institute for Lasers, Plasma and Radiation Physics, Bucharest-Magurele, Romania

3 University of Bucharest, Faculty of Physics, Bucharest-Magurele, Romania

References

[1] Socol G., Socol M., Stefan N., Axente E., Popescu-Pelin G., Craciun D., et al. Pulsed laser deposition of transparent conductive oxide thin films on flexible substrate. Applied Surface Science. 2012; **260**:42–46. DOI: 10.1016/j.apsusc.2012.02.14.

[2] Stanculescu A., Socol M., Socol G., Mihailescu I. N., Stanculescu F., Girtan M. MAPLE prepared organic heterostructures for photovoltaic applications. Applied Physics A Materials Science & Processing. 2011; **104**(3):921–928. DOI: 10.1007/s00339-011-6440-y.

[3] Ristoscu C., Gyorgy E., Mihailescu I. N., Klini A., Zorba V., Fotakis C. Effects of pulse laser duration and ambient nitrogen pressure in PLD of AlN. Applied Physics A Materials Science & Processing. 2004; **79**:927–929. DOI: 10.1007/s00339-004-2857-x.

[4] Popescu-Pelin G., Sima F., Sima L. E., Mihailescu C. N., Luculescu C., Iordache I., et al. Hydroxyapatite thin films grown by pulsed laser deposition and matrix assisted pulsed laser evaporation: comparative study. Applied Surface Science. 2016. http://dx.doi.org/10.1016/j.apsusc.2016.10.043.

[5] Girtan M. Study of charge carriers' transport in organic solar cells by illumination area shifting. Solar Energy Materials and Solar Cells. 2017; **160**:430–434. DOI: 10.1016/j.solmat.2016.11.011.

[6] Kim S. I., Lee K. W., Sahu B. B., Han J. G. Flexible OLED fabrication with ITO thin film on polymer substrate. Journal of Appied Physics. 2015; **54**:090301–090304. http://dx.doi.org/10.7567/JJAP.54.090301.

[7] Zhang L., Li J.,Zhang X. W., Jiang X. Y., Zhang Z. L. High-performance ZnO thin film transistors with sputtering $SiO_2/Ta_2O_5/SiO_2$ multilayer gate dielectric. Thin Solid Films. 2010; **518**:6130–6133. DOI: 10.1016/j.tsf.2010.06.017.

[8] Granqvist C. G., Azens A., Heszler P., Kish L. B., Österlund L. Nanomaterials for benign indoor environments: electrochromics for "smart windows," sensors for air quality, and photo-catalysts for air cleaning. Solar Energy Materials and Solar Cells. 2007; **91**:355–365. DOI: 10.1016/j.solmat.2006.10.011.

[9] Dhara A., Alforda T. L. Optimization of $TiO_2/Cu/TiO_2$ multilayer as transparent composite electrode (TCE) deposited on flexible substrate at room temperature. ECS Solid State Letters. 2014; **3**:N33–N36. DOI: 10.1149/2.0061411ssl.

[10] Chen Z., Li W., Li R., Zhang Y., Xu G., Cheng H. Fabrication of highly transparent and conductive indium-tin oxide thin films with a high figure of merit via solution processing. Langmuir. 2013; **29**:13836–13842. DOI: 10.1021/la4033282.

[11] Stanculescu A., Socol M., Rasoga O., Mihailescu I. N., Socol G., Preda N., et al. Laser prepared organic heterostuctures on glass/AZO substrates. Applied Surface Science. 2014; **302**:169–176. http://dx.doi.org/10.1016/j.apsusc.2014.01.181.

[12] Leong W. L., Ren Y., Seng H. L., Huang Z., Chiam S. Y., Dodabalapur A. Efficient polymer solar cells enabled by low temperature processed ternary metal oxide as electron transport interlayer with large stoichiometry window. ACS Applied Materials &Interfaces. 2015;**7**:11099–11106. DOI: 10.1021/acsami.5b02215.

[13] Jun M. C., Park S. U., Koh J. H. Comparative studies of Al-doped ZnO and Ga-doped ZnO transparent conducting oxide thin films. Nanoscale Research Letters. 2012; **7**:639. DOI: 10.1186/1556-276X-7-639.

[14] Liu H., Wu Z., Hu J., Song Q., Wu B., Tam H. L., et al. Efficient and ultraviolet durable inverted organic solar cells based on an aluminium doped zinc oxide transparent cathode. Applied Physics Letters. 2013; **103**:043309. DOI: 10.1063/1.4816786.

[15] Bel-Hadj-Tahar R., Mohamed A. B. Sol–gel processed indium-doped zinc oxide thin films and their electrical and optical properties. New Journal of Glass and Ceramics. 2014; **4**:55–56. http://dx.doi.org/10.4236/njgc.2014.44008.

[16] Ellmer K., Mientus R. Carrier transport in polycrystalline transparent conductive oxides: a comparative study of zinc oxide and indium oxide. Thin Solid Films. 2008; **516**:4620–4627. DOI: 10.1016/j.tsf.2007.05.084.

[17] Zhang Y., Basel T. P., Gautam B. R., Yang X., Mascaro D. J., Liu F., et al. Spin-enhanced organic bulk heterojunction photovoltaic solar cells. Nature Communications. 2012; **3**:1043. DOI: 10.1038/ncomms2057.

[18] Bhagat S. A., Borghate S. V., Kalyani N. Thejo and Dhoble S. J. Novel Na^+ doped Alq_3 hybrid materials for organic light-emitting diode (OLED) devices and flat panel displays. Luminescence. 2013; **30**:251–256. DOI: 10.1002/bio.2721.

[19] Tiwari S., Singh A. K., Prakash R. Poly(3-hexylthiophene) (P3HT)/graphene nanocomposite material based organic field effect transistor with enhanced mobility. Journal of Nanoscience and Nanotechnology. 2014; **14**:2823–2828. DOI: https://doi.org/10.1166/jnn.2014.8570.

[20] Heliatek. Heliatek sets new organic photovoltaic world record efficiency of 13.2% [Internet]. 2016. Available from: http://www.heliatek.com/en/press/press-releases/details/heliatek-sets-new-organic-photovoltaic-world-record-efficiency-of-13-2.

[21] Xie T., Xie G., Su Y., Hongfei D., Ye Z., Jiang Y. Ammonia gas sensors based on poly(3-hexylthiophene)-molybdenum disulfide film transistors. Nanotechnology. 2016; **27**:065 502. DOI: 10.1088/0957-4484/27/6/065502.

[22] Ghorannevis Z., Akbarnejad E., Elahi Salar A., Ghoranneviss M. Application of RF magnetron sputtering for growth of AZO on glass substrate. Journal of Crystal Growth. 2016; **447**:62–66. http://dx.doi.org/10.1016/j.jcrysgro.2016.04.062.

[23] Meng L. J., Gao J., Silva R. A., Song S. Effect of the oxygen flow on the properties of ITO thin films deposited by ion beam assisted deposition (IBAD). Thin Solid Films. 2008; **516**:5454–5459. DOI: 10.1016/j.tsf.2007.07.071.

[24] Yadav S. C., Uplane M. D. Synthesis and properties of Boron doped ZnO thin films by spray CVD technique at low substrate temperature. International Journal of Engineering Science and Technology. 2012; **4**:4892–4898.

[25] Socol G., Craciun D., Mihailescu I. N., Stefan N., Besleaga C., Ion L., et al. High quality amorphous indium zinc oxide thin films synthesized by pulsed laser deposition. Thin Solid Films. 2011; **520**:1274–1277. DOI: 10.1016/j.tsf.2011.04.196.

[26] Pandey R., Yuldashev S., Nguyen H. D., Jeon H. C., Kang T. W. Fabrication of aluminium doped zinc oxide (AZO) transparent conductive oxide by ultrasonic spray pyrolysis. Current Applied Physics. 2012; **12**:S56–S58. DOI: 10.1016/j.cap.2012.05.027.

[27] Girtan M., Dabos-Seignon S., Stanculescu A. On morphological, structural and electrical properties of vacuum deposited pentacene thin films. Vacuum. 2009; **83**:1159–1163. DOI: 10.1016/j.vacuum.2009.03.001.

[28] Motaung D. E., Malgasa G. F., Arendse C. J. Comparative study: the effects of solvent on the morphology, optical and structural features of regioregular poly(3-hexylthiophene):fullerene thin films. Synthetic Metals. 2010; **160**:876–882. DOI: 10.1016/j.synthmet.2010.01.038.

[29] Acikbas Y., Erdogan M., Capan R., Yukruk F. Fabrication of Langmuir–Blodgett thin film for organic vapor detection using a novel *N,N′*-dicyclohexyl-3,4:9,10-perylenebis (dicarboximide). Sensors ans Actuator B-Chemical. 2014; **200**:61–68. http://dx.doi.org/10.1016/j.snb.2014.04.051.

[30] Eggenhuisen T. M., Galagan Y., Coenen E. W. C., Voorthuijzen W. P., Slaats M. W. L., Kommeren S. A., et al. Digital fabrication of organic solar cells by Inkjet printing using non-halogenated solvents. Solar Energy Materials and Solar Cells. 2015; 1**34**: 364–372. http://dx.doi.org/10.1016/j.solmat.2014.12.014.

[31] Caricato A. P., Cesaria M., Gigli G., Loiudice A., Luches A., Martino M., et al. Poly-(3-hexylthiophene)/6,6 -phenyl-C-61-butyric-acid-methyl-ester bilayer deposition by matrix-assisted pulsed laser evaporation for organic photovoltaic applications. Applied Physics Letters. 2012;**100**:073306. DOI: 10.1063/1.3685702.

[32] Norton D. P. Pulsed laser deposition of complex materials: progress toward applications. In: Eason R.. editor. Pulsed laser deposition of thin films: applications-led growth of functional materials. 1st ed. New York, United States: Wiley & Sons; 2006. pp. 3–32. DOI: 10.1002/9780470052129.ch1.

[33] Kim H. Transparent conducting oxide films. In: Easton R., editor. Pulsed laser deposition of thin films: applications-led growth of functional materials. 1st ed.. New York, United States: John Wiley & Sons Inc. 2006. pp. 240–255. DOI: 10.1002/9780470052129.ch11.

[34] Huc I., Lehn J. M. Virtual combinatorial libraries: dynamic generation of molecular and supramolecular diversity by self-assembly. Proceeding of the National Academy of Science USA. 1997; **94**:2106–2110.

[35] Plunkett M. J., Ellman J. A. Combinatorial chemistry and new drugs. Scientific American. 1997; **276**:68–73.

[36] Sakurai J., Hata S., Yamauchi R., Shimokohbe A. Search for novel amorphous alloys with high crystallization temperature by combinatorial arc plasma deposition. Applied Surface Science. 2007; **254**:738–742. DOI: 10.1016/j.apsusc.2007.05.092.

[37] Chikyow T., Ahmeta P., Nakajimab K., Koidac T., Takakurad M., Yoshimotod M., et al. A combinatorial approach in oxide/semiconductor interface research for future electronic devices. Applied Surface Science. 2002; **189**:284–291. http://dx.doi.org/10.1016/S0169-4332(01)01004-2.

[38] Martin T. P., Chan K., Gleason K. K. Combinatorial initiated chemical vapor deposition (iCVD) for polymer thin film discovery. Thin Solid Films. 2008; **516**:681–683. DOI: 10.1016/j.tsf.2007.06.113.

[39] Socol G., Socol M., Sima L., Petrescu S., Enculescu M., Sima F., et al. Combinatorial pulsed laser deposition of Ag-containing calcium phosphate coatings. Digest Journal of Nanomaterials and Biostructures. 2012; **7**:563–576.

[40] Axente E., Socol G., Beldjilali S. A., Mercadier L., Luculescu C. R., Trinca L. M., et al. Quantitative analysis of amorphous indium zinc oxide thin films, synthesized by combinatorial pulsed laser deposition. Applied Physics A-Materials Science & Processing. 2014; **117**:229–236. DOI: 10.1007/s00339-014-8427-y.

[41] Piqué A., McGill R. A., Chrisey D. B., Leonhardt D., Mslna T. E., Spargo B. J., et al. Growth of organic thin films by the matrix assisted pulsed laser evaporation (MAPLE) technique. Thin Solid Films. 1999; **355**–**356**:536–541.

[42] Epstein A. J. and Yang Y. Polymeric and organic electronic materials: from scientific curiosity to applications. Material Research Bulletin. 1997; **22**:13–14. DOI: https://doi.org/10.1557/S0883769400033571.

[43] Luches A.,Caricato A. P. Fundamentals and applications of MAPLE. In: Miotello A., Ossi P. M., editors. Laser-surface interactions for new materials production. 1st ed.. Berlin: Springer Berlin Heidelberg; 2010. pp.203–233. DOI: 10.1007/978-3-642-03307-0_9.

[44] Caricato A. P. Lasers in materials science. MAPLE and MALDI: theory and experiments. In: Castillejo M. O., Paolo L. Zhigilei, editors. Lasers in materials science. 1st ed. Switzerland: Springer International Publishing; 2014. pp. 295–323. DOI: 10.1007/978-3-319-02898-9_12.

[45] Caricato A. P., Luches A. Applications of the matrix-assisted pulsed laser evaporation method for the deposition of organic, biological and nanoparticle thin films: a review. Applied Physics A-Materials Science & Processing. 2011; **105**(3):565–582. DOI: 10.1007/s00339-011-6600-0.

[46] Bloisi F., Barra M., Cassinese A., Vicari L. R. M. Matrix-assisted pulsed laser thin film deposition by using Nd:YAG laser. Journal of Nanomaterials. 2012; **2012**:Article ID 395436. 9 p. DOI: 10.1155/2012/395436.

[47] Socol G., Mihailescu I. N., Albu A. M., Antohe S., Stanculescu F., Stanculescu A., et al. MAPLE prepared polymeric thin films for non-linear optics applications. Applied Surface Science. 2009; **255**:5611–5614. DOI: 10.1016/j.apsusc.2008.07.206.

[48] Stadler A. Transparent conducting oxides—an up-to-date overview. Materials. 2012; **5**:661–683. DOI: 10.3390/ma5040661.

[49] van Deelen J., Illiberi A., Hovestad A., Barbu I., Klerk L., Buskens P. Transparent conducting materials: overview and recent results. SPIE. 2012; **8470**:84700-1-8. DOI: 10.1117/12.929685.

[50] Chopra K. L., Major S., Pandya D. Transparent conductors—a status review. Thin Solid Films. 1983; 1**02**:1–46. http://dx.doi.org/10.1016/0040-6090(83)90256-0.

[51] Ellmer K. Past achievements and future challenges in the development of optically transparent electrodes. Nature Photonics. 2012; **6**:809–817. DOI: 10.1038/nphoton.2012.282.

[52] Löbmann P. Transparent conducting oxides. In: Schneller T., Waser R., Kosec M., Payne D., editors. Chemical solution deposition of functional oxide thin film. 1st ed. Vienna: Springer Vienna; 2013. pp. 655–672. DOI: 10.1007/978-3-211-99311-8_26.

[53] Sohn S., Han Y. S. Transparent conductive oxide (TCO) films for organic light emissive devices (OLEDs). In: Ko S. H., editors. Organic light emitting diode—material, process and devices. 1st ed.. Rijeka, Croatia: InTech; 2011. pp. 233–274. DOI: 10.5772/18545.

[54] Paine, D. C., Yeom, H. Y., Yaglioglu, B. Transparent conducting oxide materials and technology. In: Crawford G. P., editors. Flexible flat panel displays. 1st ed. Chichester, UK: John Wiley & Sons, Ltd; 2005. DOI: 10.1002/0470870508.ch5.

[55] Ellmer K., Klein A., Rech B., editors. Transparent conductive zinc oxide. Basics and applications in thin film solar cells. 1st ed. Berlin: Springer-Verlag Berlin Heidelberg; 2008. 446 p. DOI: 10.1007/978-3-540-73612-7.

[56] Hosono H., Paine D. C., Ginley D., editors. Handbook of transparent conductors. 1st ed. US: Springer US; 2011. 534 p. DOI: 10.1007/978-1-4419-1638-9.

[57] Badeker K. Concerning the electrical conductibility and the thermoelectric energy of several heavy metal bonds. Annals of Physics. 1907; **22**:749–766.

[58] Minami T. Transparent and conductive multicomponent oxide films prepared by magnetron sputtering. Journal of Vacuum Science and Technology. 1999; **17**:1765–1772. http://dx.doi.org/10.1116/1.581888.

[59] Yanagi H., Kawazoe H., Kudo A., Yasukawa M., and Hosono H. Chemical design and thin film preparation of p-type conductive transparent oxides. Journal of Electroceramics. 2000; **4**:407–414. DOI: 10.1023/A:1009959920435.

[60] Kawazoe H., Yasukawa M., Hyodo H., Kurita M., Yanagi H., Hosono H. P-type electrical conduction in transparent thin films of $CuAlO_2$. Nature. 1997; **389**:939–942. DOI: 10.1038/40087.

[61] Kudo A., Yanagi H., Hosono H., Kawazoe H. A p-type conductive oxide with wide band gap. Applied Physics Letters. 1998; **73**:220–222. DOI: 10.1063/1.121761.

[62] Nagrajan R., Draeseke A. D., Sleight A. W., Tate J. P-type conductivity in $CuCr_{1-x}Mg_xO_2$ films and powders. Journal of Applied Physics. 2001; **89**:8022–8025. DOI: 10.1063/1.1372636.

[63] Suzuki A., Mastsushita T., Aoki T., Yoneyama Y., Okuda M. Pulsed laser deposition of transparent conducting indium tin oxide films in magnetic field perpendicular to plume. Japanese Journal of Applied Physics. 2001; **40**:L401–L403. DOI: 10.1143/JJAP.40.L401.

[64] Kim, H., Piqué A., Horwitz J. S., Mattoussi H., Murata H., Kafafi Z. H., et al. Indium tin oxide thin films for organic light-emitting devices. Applied Physics Letters. 1999; **74**:3444. DOI: 10.1063/1.124122.

[65] Jee S. H., Kim S. H., Ko J. H., Yoon Y. S. Study on work function change of ITO modified by using a self-assembled monolayer for organic based devices. Journal of the Korean Physical Society. 2006; **49**(5). 2034–2039.

[66] Kim H., Gilmore C., Piqué A., Chrisey D. B. Electrical, optical, and structural properties of indium–tin–oxide thin films for organic light-emitting devices. Journal of Applied Physics. 1999; **86**(11):6451–6461. DOI: 10.1063/1.371708.

[67] Hu J., Gordon R. G. Textured aluminium doped zinc oxide thin films from atmospheric pressure chemical vapour deposition. Journal of Applied Physics. 1992; **71**:880–890. DOI: 10.1063/1.351309.

[68] Park J. W., Kim G., Lee S. H., Kim E. H., Lee G. H. The effect of film microstructures on cracking of transparent conductive oxide (TCO) coatings on polymer substrates. Surface and Coatings Technology. 2010; **205**:915–921. http://dx.doi.org/10.1016/j.surfcoat.2010.08.055.

[69] Chung W. S., Thompson M. O., Wickboldt P., Toet D., Carey P. G. Room temperature indium tin oxide by XeCl excimer laser annealing for flexible display. Thin Solid Films. 2004; **460**:291–294. http://dx.doi.org/10.1016/j.tsf.2004.01.050.

[70] Kim H., Horwitz J. S., Kushto G. P., Kafafi Z. H., Chrisey D. B. Indium tin oxide thin films grown on flexible plastic substrates by pulsed-laser deposition for organic light-emitting diodes. Applied Physics Letters. 2001; **79**:284–286. DOI: 10.1063/1.1383568.

[71] Mekhnache M., Drici A., Saad Hamideche L., Benzarouk H., Amara A., Cattin L, et al. Properties of ZnO thin films deposited on (glass, ITO and ZnO:Al) substrates. Superlattices and Microstructures. 2011;**49**(5):510–518. http://dx.doi.org/10.1016/j.spmi.2011.02.002

[72] Fernandez S., Naranjo F. B. Optimization of aluminum-doped zinc oxide films deposited at low temperature by radio-frequency sputtering on flexible substrates for solar cell applications. Solar Energy Materials and Solar Cells. 2010; **94**:157–163. DOI: 10.1016/j.solmat.2009.08.012.

[73] Socol G., Galca A. C., Luculescu C.R., Stanculescu A., Socol M., Stefan N., et al. Tailoring of optical, compositional and electrical properties of the $In_xZn_{1-x}O$ thin films obtained by combinatorial pulsed laser deposition. Digest Journal of Nanomaterials and Biostructures. 2011; **6**(1):107–115.

[74] Girtan M., Socol M., Pattier B., Sylla M., Stanculescu A. On the structural, morphological, optical and electrical properties of sol–gel deposited ZnOIn films. Thin Solid Films. 2010; **519**(2):573–577. DOI: 10.1016/j.tsf.2010.07.006.

[75] Minami T., Kakumu T., Takeda Y., Takata S. Highly transparent and conductive ZrO-In_2O_3 thin films prepared by dc magnetron sputtering. Thin Solid Films. 1996; **291**:1–5. DOI: 10.1016/S0040-6090(96)09094-3.

[76] Moriga T., Okamoto T., Hiruta K., Fujiwara A., Nakabayashi I., Tominaga K. J. Structures and physical properties of films deposited by simultaneous DC sputtering of ZnO and In_2O_3 or ITO targets. Journal of Solid State Chemistry. 2000; **155**(2):312–331. DOI: 10.1006/jssc.2000.8919.

[77] Socol M., Preda N., Vacareanu L., Grigoras M., Socol G., Mihailescu I.N., et al. Organic heterostructures based on arylenevinylene oligomers deposited by MAPLE. Applied Surface Science. 2014; **302**:216–222. DOI: 10.1016/j.apsusc.2013.12.091.

[78] Vacareanu L., Grigoras M. Electrochemical characterization of arylenevinylene oligomers containing triphenylamine and carbazole units. Journal of Applied Electrochemistry. 2014; **40**:1967–1975. DOI: 10.1007/s10800-010-0173-z.

[79] Sakurai Y., Hosoi Y., Ishii H., Ouchi Y., Salvan G., Kobitski A., et al. Study of the interaction of *tris*-(8-hydroxyquinoline) aluminum(Alq3) with potassium using vibrational spectroscopy: examination of possible isomerization upon K doping. Journal of Applied Physics. 2004;**96**:5534–5542. http://doi.org/10.1063/1.1776626.

[80] Stanculescu A., Vacareanu L., Grigoras M., Socol M., Socol G., Stanculescu F., et al Thin films of arylenevinylene oligomers prepared by MAPLE for applications in non-linear optics. Applied Surface Science. 2011;**257**:5298–5302. DOI: 10.1016/j.apsusc.2010.11.094.

[81] Stanculescu A., Stanculescu F., Tugulea L., Socol M. Optical properties of 3,4,9,10-perylenetetracarboxylic dianhydride and 8-hydroxyquinoline aluminium salt films prepared by vacuum deposition. Material Science Forum. 2006; **514–516**:956–960.

[82] Gao Y. Surface analytical studies of interfaces in organic semiconductor devices. Materials Science and Engineering: R: Reports. 2010; **68**(3):39–87. http://dx.doi.org/10.1016/j.mser.2010.01.001.

[83] Chamberlain G. A. Organic solar cells: a review. Solar Cells. 1983; **8**(1):47–83. http://dx.doi.org/10.1016/0379-6787(83)90039-X.

[84] Stanculescu F., Rasoga O., Catargiu A. M., Vacareanu L., Socol M., Breazu C., et al. MAPLE prepared heterostructures with arylene based polymer active layer for photovoltaic applications. Applied Surface Science. 2015; **33**:240–248. DOI: 10.1016/j.apsusc.2014.11.146.

[85] Piqué A. The matrix-assisted pulsed laser evaporation (MAPLE) process: origins and future direction. Applied Physics A-Materials Science & Processing. 2011; **105**(3):517–528. DOI: 10.1007/s00339-011-6594-7.

[86] Sellinger A. T., Leveugle E., Gogick K., Peman G., Zhigilei L. V., Fitz-Gerald J. M.. Journal of Physics: Conerence Series. 2007; **59**:314–317. DOI: 10.1088/1742-6596/59/1/066.

[87] Balakrishnan K., Datar A., Zhang W., Yang X., Naddo T., Huang J., et al. Nanofibril self-assembly of an arylene ethynylene macrocycle. Journal of the American Chemical Society. 2006; **128**(20):6576–6577. DOI: 10.1021/ja0618550.

[88] Dmitruk N. L., Borkovskaya O. Yu., Havrylenko T. S., Naumenko D. O., Petrik P., Meza-Laguna V., et al. Effect of chemical modification of thin C_{60} fullerene films on the fundamental absorption edge. Semiconductor Physics, Quantum Electronics and Optoelectronics. 2010; **13**:180–185.